NADP$^+$-DEPENDENT DEHYDROGENASE ACTIVITY OF CARBONYL REDUCTASE ON GLUTATHIONYL-HYDROXYNONANAL AS A NEW PATHWAY FOR HYDROXYNONENAL DETOXIFICATION.

Roberta Moschini[a], Eleonora Peroni[a#], Rossella Rotondo[a#], Giovanni Renzone[b], Dominique Melck[c], Mario Cappiello[a], Massimo Srebot[d], Elio Napolitano[e], Andrea Motta[e], Andrea Scaloni[b], Umberto Mura[a] and Antonella Del-Corso[a*].

[a]University of Pisa, Department of Biology, Biochemistry Unit, via S. Zeno, 51, 56123, Pisa, Italy,

[b]Proteomics & Mass Spectrometry Laboratory, ISPAAM-CNR, via Argine 1085, I-80147, Napoli, Italy.

[c]Institute of Biomolecular Chemistry, ICB-CNR, Comprensorio Olivetti, Edificio A, Via Campi Flegrei 34, I-80078 Pozzuoli (Naples), Italy.

[d]Health Unit 5 Pisa, Pontedera Hospital, Ginecology and Obstetric Unit, Via Roma 180, 56025 Pontedera, Italy.

[e]Scuola Normale Superiore, Piazza dei Cavalieri, Pisa, Italy.

# These authors contributed equally to the work.

*Corresponding author: Antonella Del-Corso, University of Pisa, Department of Biology, Biochemistry Unit, via S. Zeno, 51, 56123, Pisa, Italy.

Phone: +39.050.2211454; Fax: +39.050.2211460

E-mail: antonella.delcorso@unipi.it

Abstract

A $NADP^+$ dependent dehydrogenase activity on 3-glutathionyl-4-hydroxynonanal (GSHNE) was purified to electrophoretic homogeneity from a line of human astrocytoma cells (ADF). Proteomic analysis identified this enzymatic activity as associated with carbonyl reductase 1 (E.C. 1.1.1.184). The enzyme is highly efficient at catalyzing the oxidation of GSHNE (K_M33 μM,k_{cat}405 min^{-1}), as it is practically inactive towards *trans*-4-hydroxy-2-nonenal (HNE) and other HNE-addicted thiol-containing amino acid derivatives. Combined mass spectrometry and nuclear magnetic resonance spectroscopy analysis of the reaction products revealed that carbonyl reductase oxidizes the hydroxyl group of GSHNE in its hemiacetal form, with the formation of the corresponding 3-glutathionyl-nonanoic-δ-lactone. The relevance of this new reaction catalyzed by carbonyl reductase 1 is discussed in terms of HNE detoxification and the recovery of reducing power.

Keywords: 4-hydroxy-2-nonenal; 3-glutathionyl-4-hydroxynonanal; carbonyl reductase; hydroxynonenal detoxification;

Introduction

The pathophysiological effects of oxidative stress on cells and tissues are assumed to be related, at least in part, to endogenous lipid peroxidation and to the highly reactive molecules consequently produced, of which the most abundant is *trans*-4-hydroxy-2-nonenal (HNE) [1-3]. HNE is generated as a racemic mixture of *4R*- and *4S*- enantiomers primarily from the peroxidation of ω-6 polyunsatured fatty acids [4].It may account for more than 95% of the enals produced [5,6]. Basal HNE concentrations in tissue and plasma range from 0.8 to 2.8 μM [7], and there is evidence of increased levels up to 4.5 mM in peroxidizing membranes under oxidative stress conditions [8].

HNE plays an important role in the pathogenesis of several diseases, including atherosclerosis and Alzheimer's disease [6,9,10]. The toxicity of HNE depends on its high chemical reactivity, which is associated with the presence of an aldehydic group, a double bond and a secondary alcohol at the chiral centre C_4 [11]. HNE can react with nucleophiles via 1,2 and 1,4 addition [7,12,13]. The main protein modification associated with HNE occurs via 1,4-Michael addition with Cys, Lys and His residues [7,12,14]. A number of proteins, including albumin, amyloid beta peptide, alpha-synuclein, aldose reductase and several glutathione S-transferase (GST) isoforms, have been reported to be covalently modified *in vitro* by HNE [15-25]. On the other hand, the 1,2-addition of the carbonyl group to the primary amine of Lys has also been reported, which generates the corresponding Schiff base [13,24].

As a signaling molecule, HNE is involved in modulating in a concentration-dependent manner several cellular processes, such as proliferation, differentiation and apoptosis. High concentrations of HNE have thus been reported to cause cell cycle arrest [26], differentiation [27]and apoptosis [28,29].Lower concentrations, at least in some cell types, appear to induce proliferation [30]. Intracellular control of HNE levels is thus required in order to modulate the cell cycle.

HNE metabolism involves reducing aldehyde to the corresponding 1,4 dihydroxynonene (DHN) by aldose reductase [31,32] and alcohol dehydrogenase [33,34] or oxidating aldehyde to the 4-

hydroxynonenoic acid (HNA) by aldehyde dehydrogenase [35-37]. However, the formation of the 3-glutathionyl-4-hydroxynonanal (GSHNE) is considered as the main pathway of the HNE metabolism [38-40]. GSHNE, which is present in solution essentially (95%) in its cyclic hemiacetal form [7,41], can be produced both in a spontaneous reaction between HNE and glutathione (GSH), and in a reaction efficiently catalyzed by GST [7,42]. Of the isoforms of GST in mammalian tissues, a subgroup of the α-class isozymes shows the highest catalytic efficiency for HNE [43-46].

As GSHNE is the most significant HNE derivative, its metabolism represents the main pathway for the control of HNE levels. Depletion of intracellular GSH by buthionine sulfoximine or by oxidative insult reduces GSHNE levels with a consequent increase in free HNE amounts and in cellular toxicity [47,48]. However, since GSHNE is an inhibitor of GST activity, the adduct needs to be removed from the cell by extrusion and/or intracellular metabolism [49,50].

As with HNE, GSHNE is susceptible to both oxidative and reductive transformations. Thus, aldose reductase reduces GSHNE to 1,4-dihydroxynonane-glutathione (GSDHN) [32], which has been shown to be involved in the proliferation and inflammation cell signaling cascades [51-53]. On the other hand, GSHNE can be oxidized by NAD-dependent aldehyde dehydrogenase to 4-hydroxynonanoic acid-glutathione (GSHNA) [54] or its lactone form [55]. These oxidized derivatives can be further metabolized by cytochrome P450 4A, with the subsequent production of ω-hydroxylated and carboxylated metabolites [38,55-57]. Finally, the glutathione moiety of these adducts can be transformed into mercapturic acid in the kidney and the resulting metabolites are excreted into urine [58-60].

The present study on human astrocytoma ADF cells highlights a highly efficient and specific dehydrogenase activity of carbonyl reductase 1 (CBR1) on GSHNE but not on HNE, , which was never recognized and reported before. This novel activity of CBR1 is here discussed in terms of detoxification and recovery of cell reducing power.

Materials and Methods

Materials

GSH, Cys, CysGly, γGluCys, BSA, SDS, 5,5'-dithiobis- (2-nitrobenzoic acid) (DTNB), *trans*-2-nonenal, $NADP^+$, NADPH, 9,10-PQ, and sequencing-grade trypsinwere purchased from Sigma Aldrich (St. Louis, MO, USA). 4-Oxo-nonenal (ONE), prostaglandin B_1 (PGB_1) and 4-hydroxy-2-nonenal mercapturic acid were purchased from Cayman Chemicals (Ann Arbor, MI, USA) Whatman DEAE-cellulose (DE-52) and Sephacryl S200 were purchased from GE Healthcare (Little Chalfont, UK). Blue Sepharose and Bradford reagent were purchased from Bio-Rad (Hercules, CA, USA). YM10 membranes (10kDa cut-off) were purchased from Amicon Millipore (Darmstadt, Germany). RPMI 1640, penicillin, streptomycin, glutamine and foetal bovine serum (FBS) were obtained from Lonza (Basel, Switzerland). Dialysis tubing (10kDa cut-off) was purchased from Spectrum Laboratories Inc (Rancho Dominguez, CA, USA). All inorganic chemicals were of reagent grade from BDH (VWR international ltd, Poole Dorset, UK). All solvents were HPLC-grade from J.T. Baker Chemicals (USA).

Cell cultures

ADF cells were kindly provided by Dr. W. Malorni, Istituto Superiore di Sanità, Rome, Italy.ADF cells were cultured on 10 cm diameter dishes in RPMI1640 medium supplemented with 10% (v/v) fetal bovine serum, 50 mU/mL penicillin/streptomycin and 2 mM glutamine at 37 °C, in a humidified 5% CO_2 atmosphere. Cell plates were washed with a phosphate buffer solution (PBS) (0.08% w/v NaCl, 0.002% w/v KCl, 0.002% w/v KH_2PO_4, 0.006% Na_2HPO_4), cells were harvested with a scraper and stored as suspensions in PBS (8×10^7 cells/mL) at -80°C until use.

Assay of carbonyl reductase

The activity of CBR1 was determined at 37°C using GSHNE as the substrate to be oxidized. The reaction was monitored following the increase in absorbance at 340 nm due to the reduction of $NADP^+$(ε_{340} = 6.22 $mM^{-1}\cdot cm^{-1}$). The reaction mixture contained 0.1 mM GSHNE, 0.18 mM $NADP^+$ in 50 mM sodium phosphate buffer pH 8.4. One unit of enzyme activity is the amount that catalyzes the conversion of 1 µmol of substrate/min in the above assay conditions.

The dehydrogenase activity of CBR1 was evaluated as described above on different substrates at the reported concentrations (see Results). In the case of PGB_1, 2% ethanol was present in the assay mixture. The NADPH-dependent reductase activity of CBR1was determined in the conditions described above on different substrates at the reported concentrations, following the decrease in absorbance at 340 nm due to the oxidation of 0.18 mM NADPH. In the case of 9,10-PQ and menadione, the assay mixture contained DMSO at a fixed final concentration of 2% and 1.25% (v/v), respectively. DMSO and ethanol (2% final concentration) had no effect on the activity of CBR1, as measured in standard conditions. K_M and k_{cat} values were determined by linear regression analysis of kinetic data of double reciprocal plots using GraphPad software. The k_{cat} values were calculated on the basis of a MW of 31 kDa.

Purification of the GSHNE $NADP^+$ dependent dehydrogenase activity.

A GSHNE-$NADP^+$-dependent dehydrogenase (GSHNE-DH) activity was purified from ADF cells. All procedures were carried out at 4°C. Cell lysates were obtained through a freezing and thawing protocol, followed by a centrifugation at 10,000 *x g* for 30 min. The supernatant was diluted 1:1 with4 mM DTT in10 mM sodium phosphate pH 7, and referred to as the "crude extract ".The latter was applied onto a DE-52 column (2.5x 9 cm) which was eluted with2 mM DTT in 10 mM sodium phosphate pH 7 buffer (SB) at a flow rate of 17 mL/h, collecting 3 mL fractions. SB containing 0.2 M NaCl was then applied. Fractions displaying activity were pooled and concentrated using an Amicon YM10 membrane. Thus, the concentrated protein solution was applied on a Sephacryl S200 column (1.6 x 80 cm) which was eluted with SB containing 0.1 M NaCl, at a flow rate of 20

mL/h, collecting 1.7 mL fractions. The active fractions were pooled and applied on a Blue-Sepharose column (1.2 x 8 cm), equilibrated with SB at 10 mL/h; column elution was performed with SB supplemented with 0.1 mM $NADP^+$ and NaCl at different concentrations (see details on Supplementary Materials) collecting 1.5 mL fractions. Fractions displaying GSHNE-DH activity were pooled, concentrated to a protein concentration of 0.01 mg/mL using an Amicon YM10 ultrafiltration membrane, and stored at 4°C, until used.

Synthesis of aldehydes.

Diethyl acetals of HNE and 4-hydroxy-2-noninal were prepared according to a previous procedure [61]. 4-hydroxy-2-nonanal diethyl acetal was prepared by catalytic hydrogenation (PtO in ethyl acetate) of 4-hydroxy-2-noninal diethyl acetal [62]. Free aldehydes were prepared by acid hydrolysis (pH 3.0) of the diethylacetals for 1 h, at 4°C.The concentration of HNE and *trans*-2-nonenal was determined by measuring the absorbance at 224 nm using an extinction coefficient of 13.7 $mM^{-1}\cdot cm^{-1}$ [61].

Preparation of thiol-adducts.

GSHNE, CysHNE, CysGlyHNE, and γGluCysHNE were prepared by incubating 1mM HNE in the presence of 1.5mM of each thiol containing compound in 50 mM sodium phosphate buffer pH 7.4, at 37 °C, for 1h, followed by an overnight incubation at 4 °C. The reaction was monitored by following the consumption of both HNE, by checking the absorbance at 224 nm, and of the corresponding reduced thiols by the Ellman assay [63]. Taking into account the spontaneous oxidation of the SH moiety, a stoichiometric consumption of thiols and HNE was observed in all cases. In addition, the residual HNE accounted for no more than 10% of the initial value. GS-nonanal was prepared by incubating *trans*-2-nonenal with GSH in the same conditions described above. In all cases, resulting derivatives were stored at -80°C, until used.

Proteomic identification of the GSHNE NADP$^+$ dependent dehydrogenase activity.

A protein sample exhibiting GSHNE-DH activity was analyzed by SDS-PAGE; protein bands present within the gel were excised, minced, *in gel*-reduced with DTT, S-alkylated with iodoacetamide, and digested with trypsin [64]. Resulting peptide mixtures were desalted with μZip-TipC18 (Millipore) devices, and analyzed for protein identification by nLC-ESI-LIT-MS/MS, using an LTQ XL mass spectrometer (Thermo, USA) equipped with a Proxeon nanospray source connected to an Easy-nanoLC (Thermo, USA) [65].Peptides were separated on an Easy C_{18} column (100 mm × 0.075 mm, 3 μm) (Thermo, USA);mobile phases were 0.1% v/v formic acid (solvent A) and 0.1% v/v formic acid in acetonitrile (solvent B), running at total flow rate of 300 nL/min. Linear gradient was initiated 20 min after sample loading; solvent B ramped from 5% to 35% over 45 min, from 35% to 60% over 10 min, and from 60% to 95% over 20 min. Spectra were acquired in the range *m/z* 400-2000. Peptide samples were analyzed under collision-induced dissociation-MS/MS data-dependent product ion scanning procedure, enabling dynamic exclusion (repeat count 1 and exclusion duration 60 s) over the three most abundant ions. Mass isolation window and collision energy were set to *m/z* 3 and 35%, respectively.

Raw data from nLC-ESI-LIT-MS/MS analysis were searched with a MASCOT search engine (version 2.2.06, Matrix Science, U.K.) against an updated UniProtKB non-redundant (2014/04/16) database. Database searching was performed by using a mass tolerance value of 2.0 Da for precursor ion and 0.8 Da for MS/MS fragments, trypsin as proteolytic enzyme, a missed cleavage maximum value of 2, and Cys carbamidomethylation and Met oxidation as fixed and variable modifications, respectively. Other MASCOT parameters were kept as default. Candidates with at least 2 unique assigned peptides with an individual peptide expectation value <0.05 (corresponding to a confidence level for peptide identification >95%) were considered confidently identified. Definitive peptide assignment was always associated with manual spectra verification.

Mass spectrometry analysisof the reaction products deriving from the CBR1-catalyzed oxidation of GSHNE.

A sample containing 102 μM GSHNE, 180 μM $NADP^+$, 62 μM GSH, 8.9 μM HNE in 30 mM phosphate buffer, pH 8.4, was incubated with 3.6 mU/mL CBR1, at 37 °C. The extent of reaction was monitored on a time-course basis by sampling the reaction mixture at different reaction times. Samples 1 to 4 were withdrawn at 0, 10, 40 and 80 min of incubation, respectively; sample 5 corresponded to 75 min of further incubation of the mixture after supplementation with additional enzyme (2.5 mU/mL). In parallel, identical samples containing isolated components in 30 mM phosphate buffer, pH 8.4, i.e. 102 μM GSHNE, 180 μM $NADP^+$, 62 μM GSH, 8.9 μM HNE, 3.6 mU/mL CBR1, or mixtures of that were incubated at 37 °C, as reported above. After sampling, samples were immediately frozen in dry ice, lyophilized and stored at -80 °C, until used. Samples were then solubilized in 0.1% formic acid and analyzed by nLC-ESI-LIT-MS/MS, as described above. In this case, solvent B ramped from 5% to 35% over 10 min, from 35% to 95% over 2 min. Raw data from nLC-ESI-LIT-MS/MS analyses were manually interpreted and assigned to specific glutathione derivatives.

A semi-quantitative measurement of the reaction products was obtained by analyzing the same samples with nLC-ESI-LIT-MS as described above, with the unique exception that chromatographic runs were acquired only in MS scan mode, without ion fragmentation [66, 67]. In this case, extraction and integration of the LC-MS peak areas corresponding to the reagent GSHNE and to the observed reaction products were performed in the same total ion chromatogram; the Genesis algorithm in the Xcalibur software (Thermo, USA) was used to this purpose. Since different ionization properties were expected for the different molecules, a measurement of their relative amount was obtained by extracting and integrating peak areas corresponding to these compounds and to Met-Arg-Phe-Ala (Sigma, USA); the latter peptide was used as internal reference and spiked in all samples at the same concentration before MS analysis. Semi-quantitative evaluation of the modification extent was then determined by calculating the ratio: $\text{Peak Area}_{\text{species of}}$

$_{interest}$/Peak Area$_{internal\ reference\ peptide}$. This procedure was applied to all samples reported above by performing experiments in quintuplicate.

NMR spectroscopy measurements.

For acquisition of NMR spectra, reaction samples reported in the previous section were dissolved in 30 mM sodium phosphate buffer, pH 8.4, and95% $^{1}H_2O$, 5% $^{2}H_2O$ (Cortecnet, Voisins-Le-Bretonneux, France). All spectra were recorded on a 600 MHz Bruker Avance III spectrometer (Bruker BioSpin GmbH, Rheinstetten, Germany) equipped with a CryoProbe™. One-dimensional (1D) ^{1}H-NMR spectra were collected at 300 K with the excitation sculpting pulse sequence [68] to suppress the water resonance. We used a double-pulsed field gradient echo, with a soft square pulse of 4 ms at the water resonance frequency, and the gradient pulses of 1 ms each in duration, adding 128 transients of 64k complex points, with an acquisition time of 4 s/transient. Time-domain data were all zero-filled to 128k complex points, and prior to Fourier transformation, an exponential multiplication of 0.6 Hz was applied. Two-dimensional (2D) clean total correlation spectroscopy (TOCSY) spectra [69] were recorded using a standard pulse sequence and incorporating the excitation sculpting sequence for water suppression. In general, 360 equally spaced evolution-time period t_1 values were acquired, averaging 16 transients of 2048 points with 6024 Hz of spectral width. Time-domain data matrices were all zero-filled to 4096 points in both dimensions, and prior to Fourier transformation a Lorentz-to-Gauss window was applied for both t_1 and t_2 dimensions for all the experiments. Both homonuclear 1D and 2D spectra were referred to 0.10 mM TSP, assumed to resonate at δ = 0.00 ppm in both dimensions.

For the natural abundance of 2D ^{1}H-^{13}C Heteronuclear Single Quantum Coherence (HSQC) spectra, we used an echo-antiecho phase sensitive pulse sequence using adiabatic pulses for decoupling[70].One hundred-twenty eight equally spaced evolution time period t_1 values were acquired, averaging 64 transients of 2048 points and using GARP4 for decoupling. The final data matrix was zero-filled to 4096 in both dimensions, and apodized before Fourier transformation by a

shifted cosine window function in t_2 and in t_1. Linear prediction was also applied to extend the data to twice their length in t_1. Spectra were referred to internal TSP, assumed to resonate at $\delta = 0.00$ ppm in both dimensions.

Other methods.

Protein determination was performed according to Bradford [71]. SDS-PAGE was performed according to Laemmli [72]; gels were stained by the silver stain technique [73]. The activity of aldose reductase, glucose-6-phosphate dehydrogenase, isocitrate dehydrogenase and 6-P gluconate dehydrogenase were determined at 37°C, according to [74-77], respectively.

RESULTS

Enzyme Purification and characterization. A marked $NADP^+$ reduction was observed when ADF cell crude extracts were incubated in the presence of GSHNE. This dehydrogenase activity(GSHNE-DH) was purified approximately 250-fold with an overall yield of 26%. The purification procedure included ionic exchange, exclusion and affinity chromatography. During the purification, attention was focused on discriminating between known NADP(H) oxidoreductase activities and GSHNE-DH activity. The ionic exchange step was able to separate both glucose 6-phosphate dehydrogenase and isocitric dehydrogenase from GSHNE-DH activity. The gel filtration chromatographic step separated the 6-phosphogluconate dehydrogenase from the GSHNE-DH which was significantly smaller in size (approximately 30 kDa). Finally, GSHNE-DH was separated from aldose reductase by the affinity chromatography step, giving rise to a pure GSHNE-DH preparation characterized by a protein doublet in SDS-PAGE, with an apparent molecular weight of 31-32 kDa (see the Supplementary Figures 1S-4S for chromatographic elution profiles and SDS-PAGE). The pure enzyme preparation (11 U/mg protein) was stable for at least two weeks in SB containing 0.1 mM $NADP^+$ and 1.5 M NaCl, at 4°C. Before kinetic analysis, the enzyme was

subjected to an overnight dialysis on dialysis tubing (cut off 10 kDa) against 10 mM sodium phosphate pH 7.0.

Both bands present in SDS-PAGE of the GSHNE-DH preparation (Supplementary Figure 4S) were subjected to independent proteomic analyses. Both gave the same identification results, proving their nature as 15-hydroxyprostaglandin dehydrogenase (E.C. 1.1.1.184), also referred to as carbonyl reductase 1 (CBR1). nLC-ESI-LIT-MS/MS mapping experiments provided identical results for both bands, with the exception of a peptide component uniquely observed in the case of the high mass-migrating protein component, which was associated with a CBR1 form containing a carboxyethyl mojety at Lys238 (see the Supplementary Fig. 5S for the MS/MS spectrum of the modified peptide). This component was absent in the low mass-migrating protein component, which conversely showed the presence of the corresponding non-modified counterpart (data not shown).

NADP(H) dependent activity of CBR1fromADF cells. The NADPH-dependent reductase activity of the purified CBR1 was tested on a number of molecules, including classical substrates of this enzyme (Table 1). Of these, only 9,10-PQ, menadione and ONE, in the order of decreasing effectiveness, were reduced by the enzyme, while different alkenals and their glutathionyl derivatives (including GSHNE) were completely unaffected. The kinetic parameters evaluated for the NADPH-dependent reduction of 9,10-PQ (1.8 ± 0.2 μM and 101 ± 4 min^{-1}, for K_M and k_{cat}, respectively, Fig. 1) were in accordance with the literature data reported for human CBR1 [78]. Also the $NADP^+$-dependent dehydrogenase activity of the enzyme was tested on a number of molecules (Table 2), including PGB_1, a distinctive substrate for the dehydrogenase action of CBR1 [79] and GSHNE, which was used in this study to monitor enzyme purification. Of the tested substrates, only GSHNE and PGB_1 were transformed. No effect on the enzyme activity was observed when either N-acetyl cysteine or buthionine sulfoximine were present in the assay mixture at the final concentration of 0.5 mM.

The reaction was strictly dependent on $NADP^+$ since NAD^+ was completely ineffective as a cofactor for all the tested substrates. The same pattern of dehydrogenase activity towards pyridine cofactors and different substrates was observed with a recombinant CBR1 obtained from RNA isolated from ADF cells. It is worth noting that the cDNA sequence obtained for the ADF enzyme completely matched with the human wild type sequence.

$NADP^+$-dependent GSHNE-DH activity of CBR1. A comparative kinetic analysis between GSHNE and PGB_1 revealed that the former was a far better substrate for the enzyme than the one considered as its distinctive substrate (Fig. 2). In the case of GSHNE oxidation, a K_M of 33 ± 2 μM and a k_{cat} of 405 ± 7 min^{-1} were measured; for PGB_1 a K_M of 91 ± 8 μM and a k_{cat} of 60 ± 2 min^{-1} were obtained. Thus, the specificity constant (k_s) for GSHNE (12.3 x 10^3 ± 0.7 x 10^3 mM^{-1} min^{-1}) was approximately 18 fold higher than for PGB_1 (0.7 x10^3 ± 0.1 x 10^3 mM^{-1} min^{-1}). In addition, while a 40% decrease in activity was observed with PGB_1 when the pH of the reaction buffer was decreased from 8.4 to 7.4, no changes in activity (a less than 10% decrease) were observed when GSHNE was used as substrate in the pH range 8.4-6.4.

The effectiveness of $NADP^+$ as a cofactor for the GSHNE oxidation is reported in Fig. 3. CBR1 displayed a K_M value for the cofactor of 11 ± 2μM and a k_{cat} value of 367 ± 17 min^{-1}, which accounted for a k_s value equal to 33.4 x 10^3 ± 5.9 x 10^3 $mM^{-1}min^{-1}$. Figure 3 also reports the effect of both NAD^+ and NADPH on the GSHNE oxidation. There was an apparent competitive inhibitory effect of NADPH on the dehydrogenase reaction (K_i value approximately equal to 6 μM). In addition, NAD^+, which cannot be used as a cofactor by the enzyme, failed to interfere with the $NADP^+$ dependent dehydrogenase reaction.

Identification of the reaction products by nLC-ESI-LIT-MS/MS. Analysis of the reaction products of the GSHNE oxidation catalyzed by CBR1 was performed on samples taken from a transformation time curve of the substrate at 37°C, as deriving from a mixture containing 102 μM

GSHNE, 180 μM $NADP^+$ and 3.6 mU/mL of purified CBR1in 30 mM sodium phosphate pH 8.4. The mixture also contained GSH and HNE (62 μM and 8.9 μM, respectively) as residual reagents of the GSHNE preparation; both compounds had been previously verified not to affect the enzyme activity. The increase in absorbance at 340 nm (linked to $NADP^+$ reduction) was monitored; samples at 0, 10, 40 and 80 min of incubation (samples 1 to 4, respectively) were withdrawn as reported in the experimental section. Under these conditions, the extent of $NADP^+$ reduction accounted for approximately 40 μM, which increased to 52 μM after 75 min of further incubation of the mixture after supplementation with additional 2.5 mU/mL of the enzyme (sample 5). All samples were then analyzed by nLC-ESI-LIT-MS/MS and NMR.

nLC-ESI-LIT-MS/MS analysis of standard compounds and the reaction mixtures mentioned above (samples 1 to 5) identified initial reagents and glutathione derivatives that progressively appeared after the addition of CBR1. A number of peaks showing the same mass value were observed in the nLC-ESI-LIT-MS/MS profile that, considering the occurrence of various chiral centers in these HNE-addicted glutathione derivatives, were associated with pairs of unresolved diastereomers (see the Supplementary Fig. 6S for the total ion current and ion-extracted chromatograms of sample 4), as already reported in the case of GSHNE [80,81] and other HNE-thiol adducts [82,83]. The most representative peaks referred to GSHNE (exp. and theor. MH^+ values at *m/z*464.18 and 464.21, respectively) (Fig. 4A), which was originally present in the mixture before CBR1 addition and decreased during the incubation with the enzyme (Fig. 5), and to glutathione derivatives showing an experimental MH^+ signal at about *m/z*462.23, namely glutathionyl-4-ketononanal or glutathionyl-4-hydroxynonanoic acid (GSHNA) δ-lactone (theor. MH^+ value at *m/z*462.19) (Fig. 4B), which increased on a time-course basis (Fig. 5). Less significant was the generation of GSHNA in its acyclic form (exp. and theor. MH^+ values at *m/z*480.25 and 480.20, respectively) (Fig. 4C), and even less the generation of the double-centered oxidative product glutathionyl-4-ketononanoic acid (exp. and theor. MH^+ values at *m/z*478.19 and 478.19, respectively) (Fig. 5). Semi-quantitative measurements of the reaction mixtures assumed that all HNE-addicted glutathione derivatives

reported in this study might present the same ionization tendency. According to the nature of the products observed during time-course nLC-ESI-LIT-MS/MS analysis of the incubation mixtures, a reaction pathway catalyzed by CBR1 was proposed (Fig. 6).

Characterization of the reaction products by NMR analysis. The nature of the initial reagents and of the resulting product(s) was finally demonstrated by NMR analysis. We firstly analyzed single products and their mixtures without CBR1. Resonances were assigned using 2D homo- and heteronuclear experiments. In the GSHNE/GSH/HNE and GSHNE-GSH-HNE-$NADP^+$ spectra (Fig. 7), the envelope centered at 5.57 ppm was assigned to 1-H of GSHNE and was consistent with the occurrence of the cyclic hemiacetal form of HNE adducts [81] under the experimental conditions we used. Four peaks (I at 5.59 ppm, II at 5.53 ppm, III at 5.50 ppm, and IV at 5.47 ppm) were identified. They stem from the four major diastereomers of the spontaneous reaction of racemic HNE with GSH. Considering the chiral centers, there are eight potential GSHNE diastereomers in total, and it is possible that each of the four peaks constitute a pair of unresolved diastereomers [81]. The remaining proton signals of GSHNE were also identified and are indicated in Fig. 7 (middle and upper spectra).

Analysis of the low field region of the reaction time course in phosphate buffer (Fig. 8) indicated that, in the presence of CBR1, peaks I-IV originating from proton 1 of GSHNE started to be modified after 10 min, with all NADPH peaks appearing and the corresponding reduction of $NADP^+$ signals. After 80 min, peaks II, III and IV almost disappeared, while peak I was still partially present, with the doublet at 5.50 ppm originating from NADPH. After 155 min (top spectrum),peak I was barely visible. Analysis of the high-field region between 2.5 and 2.3 ppm clarified the presence of the GSHNA δ-lactone (Fig. 9). In fact, formation of lactone requires disappearance of proton 1(Fig.6); this can be followed in the evolution of the GSHNE signals labeled 2 in Fig. 9. The ongoing reaction from 10 to 155 min indicated that the multiplicity of

proton 2 changed from a multiplet (at 10 min) to become a double doublet (at 80 min). This multiplicity was only due to the coupling with proton 3, while coupling with proton 1 was removed by the lactone formation. The combined characterization through MS and NMR approaches of the initial reagent, in its hemiacetal form, and of the product(s) resulting as result of the CBR1-catalyzed process clarified the reaction pathway as mainly yielding glutathionyl-4-hydroxynonanoic acid δ-lactone.

DISCUSSION

An assessment of the rational basis for the multiplicity of the effects exerted by HNE [26-30]entails defining all its metabolic pathways and understanding their importance. Although various enzymes are known to directly intervene on HNE, the main step of its detoxification (both in the reductive and in the oxidative direction) appears to be mediated by the conjugation with GSH [3], which can occur spontaneously or catalyzed by glutathione transferase (GST) isoforms [7,42].

Since GSHNE is the most abundant HNE derivative, its metabolism represents the main pathway for the control of HNE levels. In this context, GSHNE can be reduced to GS-DHN by aldose reductase or oxidized to GSHNA and GSHNA lactone by NAD-dependent aldehyde dehydrogenase [54,55]. The data reported in this study add a novel element to this scenario, and demonstrate that GSHNE can also be efficiently oxidized to GSHNA lactone by carbonyl reductase 1 (CBR1), a well-represented NADP(H)-dependent enzyme in various human cells [78,85]. This enzyme has been already reported to catalyze the NADPH-dependent reduction of different endogenous and xenobiotic carbonyl compounds [86], including 4-oxononenal (ONE) and its glutathione adduct (GS-ONE) [87], thus playing an active role against oxidative stress, neurodegeneration and apoptosis [88-92]. However, except for the glutathionyl-NO adduct, endogenous substrate(s) of CBR1 have not been successfully identified [93].

The protocol optimized for the purification of this GSHNE $NADP^+$ dependent dehydrogenase activity from ADF cells led to the isolation of two protein species, migrating with apparent mass of

31-32 kDa in SDS-PAGE (see Supplementary Fig. 4S). Proteomic analysis identified both proteins as human CBR1, also known as $NADP^+$ 15-hydroxyprostaglandine dehydrogenase, and proved their migration differences due to the occurrence of a carboxyethyl mojety at Lys238 (see Supplementary Fig. 5S).This modification has been already described for the human enzyme and has been demonstrated to have no effect on the protein activity and specificity [94,95].

The enzyme isolated from ADF cells acts on classical substrates of CBR1, as it is able to reduce 9,10-PQ, menadione and ONE (Table 1, Fig. 1) and also to oxidize PGB_1 (Table 2). A kinetic characterization of the ADF GSHNE-DH activity using both PGB_1 and GSHNE as substrates (Fig.2) revealed a significantly higher efficiency of the enzyme for GSHNE, for which a specificity constant was found (12.3×10^3 mM^{-1} min^{-1}) that was approximately 18-fold higher than PGB_1. The reduction of prostaglandin A_1 by CBR1 has already been reported to be positively affected by the presence of a glutathionyl moiety on the molecule [85], which may explain the marked difference reported here between GSHNE and PGB_1 as substrates to be oxidized. In any case, GSHNE was readily and efficiently oxidized by CRB1 in a wide range of pH values (6.5-8.4).

The time-course evolution of the oxidative products of GSHNE was revealed by a combined MS and NMR approach (Figures 4, 5, 7, 8 and 9). The problem of attributing the most abundant reaction product with MH^+signal at *m/z*462.23 (Fig. 4B) at the end of the reaction to either glutathionyl-4-ketononanal or glutathionyl-4-hydroxynonanoic acid δ-lactone was solved by NMR, which indicated the latter as the main oxidation derivative. In this context, time-course analysis of peaks I-IV in NMR spectra (Fig. 8) suggests that II-IV disappeared at the end of the incubation, while peak I was still visible. This could indicate that three diastereomers react faster than the one corresponding to peak I. According to the chemical shift values previously reported by Balogh et al. [81], the lowest-field signal resonating at 5.59 ppm by analogy should correspond to 3*S*,4*R*-GSHNE. Accordingly, we can speculate that the latter species does not properly fit into the CBR1 active site. A similar condition of diastereoisomer-oriented GSHNE oxidation was also observed during nLC-ESI-LIT-MS/MS analysis of the reaction products (see Supplementary Fig. 6S).

To our knowledge, only one study has reported evidences of a $NADP^+$-dependent oxidation of GSHNE as catalyzed by recombinant ALDH3A1 [54]. This enzyme, however, is mainly active on HNE and, only to a lesser extent, on GSHNE. On the other hand, the specificity displayed by CRB1 towards GSHNE with respect to HNE is worth noting, according to the data reported in this study, as the latter compound is not processed at all by the enzyme. The identification of GSHNA-δ-lactone as the main reaction product gives a first conceivable rationale basis for the selective recognition of GSHNE by CBR1. Product analysis, in fact, indicates the hydroxyl group of the hemiacetal form of the glutathionyl-derivative as a reactive center. This hydroxyl group is derived from a structural rearrangement that HNE fails to undergo because of the *trans* disposition of C4-hydroxyl and C1-carbonyl groups. However, the occurrence of a hemiacetal hydroxyl group seems not a sufficient requirement for enzyme action, since 4-hydroxynonanal, a molecule competent for cyclic hemiacetal formation, was not recognized as a substrate (Table 2). These results confirmed the importance of the glutathionyl-moiety in tailoring good substrates for CBR1 [85], as it occurs for GSHNE. The occurrence of structural restrictions exerted by the glutathionyl moiety present on substrates is underlined by the complete lack of action of CBR1 on other HNE-addicted thiol-containing amino acid and dipeptide substrates, which were tested for the enzyme dehydrogenase activity (Table 2). Furthermore, the inability of the enzyme to oxidize GS-nonanal (Table 2) indicates that CBR1 does not recognize a substrate containing a free carbonyl moiety, but the occurrence of a hemiacetal structure is also required.

The formation of GSHNA lactone was reported also to occur when GSHNE was incubated with cytosolic fractions of murine liver and kidney [55]. On the basis of an experimental inhibition of GSHNE oxidation by disulfiram, the oxidative metabolism of GSHNE was associated with a NAD^+ dependent aldehyde dehydrogenase activity [55]. However, this observation was misleading since disulfiram is not a selective inhibitor of ALDHs, but also inhibits CBR1 [96]. Indeed, we have measured a 32% inhibition of the purified ADF GSHNE DH activity in the presence of 20 μM disulfiram, when the assay was performed in standard assay conditions (data not shown). In

addition, in dialyzed rat liver extracts GSHNE appears to be oxidized through both a NAD^+ and a $NADP^+$-dependent reaction (R. Moschini and R. Rotondo, 2014, unpublished results). Finally, a $NADP^+$ dehydrogenase activity on GSHNE has recently been found also in human placental, bovine kidney and rat testis dialyzed crude extracts (R. Moschini and R. Rotondo, 2014, unpublished results).

As generally occurs with other oxidoreductases, CBR1 efficiently and specifically recognizes $NADP^+$ as a cofactor with a K_M of 11 μM (Fig. 3). However, the apparent inhibitory effect exerted by NADPH on GSHNE oxidation, especially at the $NADP^+$/NADPH ratios present *in vivo*, raises the question on the functional involvement of the GSHNE-DH activity of CBR1 in the GSHNE antioxidant metabolic pathways. In fact, the low $NADP^+$/NADPH ratio values generally present in normal healthy cells would suggest that CBR1 does not act as a dehydrogenase. However, this condition does not concur in cancer cells, where high (or very high) $NADP^+$/NADPH ratios have generally been measured. For example, PC3 human prostate cancer cells present a $NADP^+$/NADPH value of 2.2, which reaches the apex of 6.5 under glucose deprivation conditions [97]. Similarly, breast and colon cancer cells show $NADP^+$/NADPH ratios equal to 5 and 1, respectively, which dramatically increase under glucose deprivation conditions in which NADPH became practically undetectable [98]. In addition, mutated forms of both the mitochondrial and cytosolic isoforms of NADP-dependent isocitrate dehydrogenase, diffusely occurring in glioma and acute myeloid leukaemia cells, channel the α–ketoglutarate (formed with the concomitant generation of NADPH) towards the formation of 2-hydroxyglutarate with NADPH consumption [99].

All these evidences support our proposal for the possible entrance of CBR1 in the enzyme pattern (i.e. the pentose phosphate pathway enzymes, isocitrate and malate dehydrogenases) aimed at rebuilding the cell-reducing conditions through the NADPH recovery. This role, which seems to take place in cancer cells, may also more generally apply to biological systems undergoing oxidative stress, where lipid peroxidation takes place. In this context, CBR1 should play a dual role in HNE detoxification and in the recovery of the cellular reducing power. In conclusion, the

efficient and specific $NADP^+$-dependent oxidation of GSHNE to GSHNA-δ-lactone catalyzed by CBR1, as shown in this study, suggests another way in HNE breakdown, thus leading to the possibility of identifying new strategies for the modulation of the HNE metabolism.

Acknowledgements. This work was supported in part by MIUR, PRIN Project 2009M8FKBB_003 and in part by the University of Pisa.

References

[1] Parola, M.; Bellomo, G.; Robino, G.; Barrera, G.; Dianzani, M.U. 4-Hydroxynonenal as a biological signal: molecular basis and pathophysiological implications. *Antioxi. Redox Signal.* 1: 255-284; 1999.

[2] Dianzani, M.U. 4-Hydroxynonenal from pathology to physiology. *Mol. Aspects Med.* 24: 263-272; 2003.

[3] Dalleau, S.; Baradat, M.; Guéraud, F.; Huc, L. Cell death and diseases related to oxidative stress: 4-hydroxynonenal in the balance. *Cell Death Differ.* 20: 1615-1630; 2013.

[4] Schneider, C.; Tallman, K.A.; Porter, N.A.; Brash, A.R. Two distinct pathways of formation of 4-hydroxynonenal. Mechanism of nonenzymatic transformation of the 9- and 13- hydroperoxides of linoleic acid to 4-hydroxyalkenals. *J. Biol. Chem.* 276: 20831-20838; 2001.

[5] Benedetti, A.; Comporti, M.; Esterbauer, H. Identification of 4-hydroxynonenal as a cytotoxic product originating from the peroxidation of liver microsomal lipids. *Biochim. Biophys. Acta* 620: 281-296; 1980.

[6] Uchida, K. 4-Hydroxy-2-nonenal: a product and mediator of oxidative stress. *Prog. Lipid Res.* 42: 318-343; 2003.

[7] Esterbauer, H.; Schaur, R.J.; Zollner, H. Chemistry and biochemistry of 4-hydroxynonenal, malonaldehyde and related aldehydes. *Free Radic. Biol. Med.* 11: 81-128; 1991.

[8] Benedetti, A.; Comporti, M.; Fulceri, R.; Esterbauer, H. Cytotoxic aldehydes originating from the peroxidation of liver microsomal lipids. Identification of 4,5-dihydroxydecenal. *Biochim. Biophys. Acta* 792: 172-181; 1984.

[9] Liu, Q.; Raina, A.K.; Smith, M.A.; Sayre, L.M.; Perry, G. Hydroxynonenal, toxic carbonyls, and Alzheimer disease. *Mol. Aspects Med.* 24: 305-313; 2003.

[10] Picklo, M.J.; Montine, T.J.; Amarnath, V.; Neely, M.D. Carbonyl toxicology and Azheimer's disease. *Toxicol. Appl. Pharmacol.* 184: 187-197; 2002.

[11] Schaur, R.J. Basic aspects of the biochemical reactivity of 4-hydroxynonenal. *Mol. Aspects Med.* 24: 149-159; 2003.

[12] Nadkarni, D.V.; Sayre, L.M. Structural definition of early lysine and histidine adduction chemistry of 4-hydroxynonenal. *Chem. Res. Toxicol.* 8: 284-291; 1995.

[13] Wade, L.G., Jr. *Organic chemistry*, 5th ed. Upper Saddle River, NJ: Prentice-Hall; 2003: 1042-1045.

[14] Doorn, J.A.; Petersen, D.R. Covalent modification of amino acid nucleophiles by the lipid peroxidation products 4-hydroxy-2-nonenal and 4-oxo-2-nonenal. *Chem. Res. Toxicol.* 15: 1445-1450; 2002.

[15] Aldini, G.; Gamberoni, L.; Orioli, M.; Beretta, G.; Regazzoni, L.; Maffei Facino, R.; Carini, M. Mass spectrometric characterization of covalent modification of human serum albumin by 4-hydroxy-*trans*-2-nonenal. *J. Mass. Spectrom.* 41: 1149-1161; 2006.

[16] Szapacs, M.E.; Riggins, J.N.; Zimmerman, L.J.; Liebler, D.C. Covalent adduction of human serum albumin by 4-hydroxy-2-nonenal: kinetic analysis of competing alkylation reactions. *Biochemistry* 45: 10521-10528; 2006.

[17] Magni, F.; Galbusera, C.; Tremolada, L.; Ferrarese, C.; Kienle, M.G. Characterisation of adducts of the lipid peroxidation product 4-hydroxy-2-nonenal and amyloid beta-peptides by liquid chromatography/electrospray ionization mass spectrometry. *Rapid Commun. Mass Spectrom.* 16: 1485-1493; 2002.

[18] Siegel, S.J.; Bieschke, J.; Powers, E.T.; Kelly, J.W. The oxidative stress metabolite 4-hydroxynonenal promotes Alzheimer protofibril formation. *Biochemistry* 46: 1503-1510; 2007.

[19] Qin, Z.; Hu, D.; Han, S.; Reaney, S.H.; Di Monte, D.A.; Fink, A.L. Effect of 4-hydroxy-2-nonenal modification on alpha-synuclein aggregation. *J.Biol.Chem.* 282: 5862-5870; 2006.

[20] Del Corso, A.; Dal Monte, M.; Vilardo, P.G.; Cecconi, I.; Moschini, R.; Banditelli, S.; Cappiello, M.; Tsai, L.; Mura, U. Site-specific inactivation of aldose reductase by 4-hydroxynonenal. *Arch. Biochem. Biophys.*350: 245-248; 1998.

[21] Mitchell, A.E.; Morin, D.; Lamé, M.W.; Jones, A.D. Purification, mass spectrometric characterization, and covalent modification of murine glutathione S-transferases. *Chem. Res. Toxicol.* 8: 1054-1062; 1995.

[22] van Iersel, M.L.; Ploemen, J.P.; Lo Bello, M.; Federici, G.; van Bladeren, P.J. Interactions of alpha, beta-unsatured aldehydes and ketones with human glutathione S-transferase P1-1. *Chem. Biol. Interact.* 108: 67-78; 1997.

[23] Shireman, L.M.; Kripps, K.A.; Balogh, L.M.; Conner, K.P.; Whittington, D.; Atkins, W.M. Glutatione transferase A4-4 resists adduction by 4-hydroxynonenal. *Arch. Biochem. Biophys.* 504: 182-189; 2010.

[24] Bachi, A.; Dalle Donne, A.; Scaloni, A. Redox proteomics chemical principles, methodological approaches and biological/biomedical promises. *Chem. Rev.* 113: 596-698; 2013.

[25] Dalle-Donne I.; Scaloni, A.; Giustarini, D.; Cavarra, E.; Tell, G.; Lungarella, G.; Colombo, R.; Rossi, R.; Milzani, A. Proteins as biomarkers of oxidative/nitrosative stress in diseases: the contribution of redox proteomics. *Mass Spectrom Rev.* 24: 55-99; 2005.

[26] Wonisch, W.; Kohlwein, S.D.; Schaur J.; Tatzber, F.; Guttenberger, H.; Zarkovic, N.; Winklen, R. Treatment of the budding yeast *Saccharomyces cerevisiae* with the lipid peroxidation product 4-HNE provokes a temporary cell cycle arrest in G_1 phase. *Free Rad. Biol. Med.* 25: 682-687; 1998.

[27] Cheng, J.Z.; Singhal, S.S.; Saini, M.; Singhal, J.; Piper, J.T.; Van KuijK, F.J.; Zimniak, P.; Awasthi, Y.C.; Awasthi, S. Effects of mGST A4 transfection on 4-hydroxynonenal-mediated apoptosis and differentiation of K562 human erythroleukemia cells. *Arch. Biochem. Biophys.* 372: 29-36; 1999.

[28] Camandola, S.; Poli, G.; Mattson, M.P. The lipid peroxidation product 4-hydroxy-2,3-nonenal increases AP-1-binding activity through caspase activation in neurons. *J. Neurochem.* 74: 159-168; 2000.

[29]Ji, C.; Amarnath, V.; Pietenpol, J.A.; Marnett, L.J. 4-Hydroxynonenal induces apoptosis via caspase-3 activation and cytochrome c release. *Chem. Res. Toxicol.* 14: 1090-1096; 2001.

[30] Ruef, J.; Rao, G.N.; Li, F.; Bode, C.; Patterson, C.; Bhatnagar, A.; Runge, M.S. Induction of rat aortic smooth muscle cell growth by the lipid peroxidation product 4-hydroxy-2-nonenal. *Circulation* 97:1071-1078¸1998.

[31] Vander Jagt, D.L.; Kolb, N.S.; Vander Jagt, T.J.; Chino, J.; Martinez, F.J.; Hunsaker, L.A.; Royer, R.E. Substrate specificity of human aldose reductase: identification of 4-hydroxynonenal as an endogenous substrate. *Biochim. Biophys. Acta* 1249; 117-126; 1995.

[32] Srivastava, S.; Chandra, A.; Bhatnagar, A.; Srivastava, S.K.; Ansari, N.H. Lipid peroxidation product, 4-hydroxynonenal and its conjugate with GSH are excellent substrates of bovine lens aldose reductase. *Biochem. Biophys. Res. Commun.* 217: 741-746; 1995.

[33] Canuto, R.A.; Muzio, G.; Maggiora, M.; Poli, G.; Biasi, F.; Dianzani, M.U.; Ferro, M.; Bassi, A.M.; Penco, S.; Marinari, U.M. Ability of different hepatoma cells to metabolize 4-hydroxynonenal. *Cell Biochem. Funct.* 11: 79-86; 1993.

[34] Hartley, D.P.; Ruth, J.A.; Petersen, D.R. The hepatocellular metabolism of 4-hydroxynonenal by alcohol dehydrogenase, aldehyde dehydrogenase, and glutatione S-transferase. *Arch. Biochem. Biophys.* 316: 197-205.

[35] Pappa, A.; Estey, T.; Manzer, R.; Brown, D.; Vasiliou, V. Human aldehyde dehydrogenase 3A1 (ALDH3A1): biochemical characterization and immunohistochemical localization in the cornea. *Biochem. J.* 376: 615-623: 2003.

[36] Murphy, T.C.; Amarnath, V.; Gibson, K.M.; Picklo, M.J. Sr. Oxidation of 4-hydroxy-2-nonenal by succinic semialdehyde dehydrogenase (ALDH5A). *J. Neurochem.* 86: 298-305; 2003.

[37] Kong, D.; Kotraiah, V. Modulation of aldehyde dehydrogenase activity affects (±)-4-hydroxy-2E-nonenal (HNE) toxicity and HNE-protein adducts levels in PC12 cells. *J. Mol. Neurosci.* 47: 595-603; 2012.

[38] Alary, J.; Guéraud, F.; Cravedi, J.P. Fate of 4-hydroxynonenal in vivo: disposition and metabolic pathways. *Mol. Aspects Med.* 24: 177-187; 2003.

[39] Awasthi, Y.C.; Ansari, G.A.; Awasthi, S. Regulation of 4-hydroxynonenal mediated signaling by glutathione S-transferases. *Methods Enzymol.* 401: 379-407; 2005.

[40] Boon, P.J.; Marinho, H.S.; Oosting, R.; Mulder, G.J. Glutathione conjugation of 4-hydroxy-*trans*-2,3-nonenal in the rat in vivo, the isolated perfused liver and erythrocytes. *Toxicol. Appl. Pharmacol.* 159: 214-223; 1999.

[41] Esterbauer, H.; Zollner, H.; Scholz, N. Reaction of glutathione with conjugated carbonyls. *Z. Naturforsch C.* 30: 466-473; 1975.

[42] Guéraud, F.; Atalay, M.; Bresgen, N.; Cipak, A.; Eckl, P.M.; Huc, L.; Jouanin, I.; Siems, W.; Uchida, K. Chemistry and biochemistry of lipid peroxidation products. *Free Radic. Res.* 44: 1098-1124; 2010.

[43] Zimniak, P.; Singhal, S.S.; Srivastava, S.K.; Awasthi, S.; Hayden, J.B.; Awasthi, Y.C. Estimation of genomic complexity, heterologous expression, and enzymatic characterization of mouse glutathione S-transferase mGSTA4-4 (GST 5.7). *J. Biol. Chem.* 269: 992-1000; 1994.

[44] Singhal, S.S.; Awasthi, S.; Srivastava. S.K.; Zimniak, P.; Ansari, N.H.; Awasthi, Y.C. Novel human ocular glutathione S-transferases with high activity toward 4-hydroxynonenal. *Invest. Ophathalmol. Vis. Sci.* 36: 142-150; 1995.

[45] Hubatsch, I.; Ridderström, M.; Mannervik, B. Human glutathione transferase A4-4: an alpha class enzyme with high catalytic efficiency in the conjugation of 4-hydroxynonenal and other genotoxic products of lipid peroxidation. *Biochem. J.* 330: 175-179; 1998.

[46] Balogh, L.M.; Le Trong, I.; Kripps, K.A.; Shireman, L.M.; Stenkamp, R.E.; Zhang, W.; Mannervik, B.; Atkins, W.M. Substrate specificity combined with stereopromiscuity in glutathione transferase A4-4-dependent metabolism of 4-hydroxynonenal. *Biochemistry* 49: 1541-1548; 2010.

[47] Yadav, U.C.; Ramana, K.V.; Awasthi, Y.C.; Srivastava, S.K. Glutathione level regulates HNE-induced genotoxicity in human erythroleukemia cells. *Toxicol. Appl. Pharmacol.* 227: 257-264; 2008.

[48] Aldini, G.; Granata, P.; Marinello, C.; Beretta, G.; Carini, M.; Facin, R.M. Effects of UVB radiation on 4-hydroxy-2-*trans*-nonenal metabolism and toxicity in human keratinocytes. *Chem. Res. Toxicol.* 20: 416-423; 2007.

[49] Ishikawa, T.; Esterbauer, H.; Sies, H. Role of cardiac glutathione transferase and of the glutathione S-conjugate export system in biotransformation of 4-hydroxynonenal in the heart. *J. Biol. Chem.* 261: 1576-1581; 1986.

[50] Sharma, R.; Yang, Y.; Sharma, A.; Dwivedi, P.; Popov, V.L.; Boor, P.J.; Singhal, S.S.; Awasthi, S.; Awasthi, Y.C. Mechanisms and physiological significance of the transport of the glutathione conjugate of 4-hydroxynonenal in human lens ephitelial cells. *Invest. Ophathalmol. Vis. Sci.* 44: 3438-3449; 2003.

[51] Ramana, K.V.; Bhatnagar, A.; Srivastava, S.; Yadav, U.C.; Awasthi, S.; Awasthi, Y.C.; Srivastava, S.K. Mitogenic responses of vascular smooth muscle cells to lipid peroxidation-derived aldehyde 4-hydroxy-*trans*-2-nonenal (HNE): role of aldose reductase-catalyzed reduction of the HNE-glutathione conjugates in regulating cell growth. *J. Biol. Chem.* 281: 17652-17660; 2006.

[52] Srivastava, S.; Ramana, K.V.; Bhatnagar, A.; Srivastava, S.K. Synthesis, quantification, characterization, and signaling properties of glutathionyl conjugates of enals. *Methods Enzymol.* 474: 297-313; 2010.

[53] Ramana, K.V.; Fadl, A.A.; Tammali, R.; Reddy, A.B.; Chopra, A.K.; Srivastava, S.K. Aldose reductase mediates the lipopolysaccharide-induced release of inflammatory mediators in RAW264.7 murine macrophages. *J. Biol. Chem.* 281: 33019-33029; 2006.

[54] Black, W.; Chen, Y.; Matsumoto, A.; Thompson, D.C.; Lassen, N.; Pappa, A.; Vasiliou, V. Molecular mechanisms of ALDH3A1-mediated cellular protection against 4-hydroxy-2-nonenal. *Free Rad. Biol. Med.* 52: 1937-1944; 2012.

[55] Alary, J.; Fernandez, Y.; Debrauwer, L.; Perdu, E.; Guéraud, F. Identification of intermediate pathways of 4-hydroxynonenal metabolism in the rat. *Chem. Res. Toxicol.* 16: 320-327; 2003.

[56] Alary, J.; Debrauwer, L.; Fernandez, Y.; Paris, A:; Cravedi, J.P.; Dolo, L.; Rao, D.; Bories, G. Identification of novel urinary metabolites of the lipid peroxidation product 4-hydroxy-2-nonenal in rats. *Chem. Res. Toxicol.* 11: 1368-1376; 1998.

[57] Guéraud, F.; Alary, J.; Costet, P.; Debrauwer, L.; Dolo, L.; Pineau, T.; Paris, A. In vivo involvement of cytochrome P450 4A family in the oxidative metabolism of the lipid peroxidation product *trans*-4-hydroxy-2-nonenal, using PPARalpha-deficient mice. *J. Lipid. Res.* 40: 152-159; 1999.

[58] Alary, J.; Bravais, F.; Cravedi, J.P.; Debrauwer, L.; Rao, D.; Bories, G. Mercapturic acid conjugates as urinary end metabolites of the lipid peroxidation product 4-hydroxy-2-nonenal in the rat. *Chem. Res. Toxicol.* 8: 34-39; 1995.

[59] de Zwart, L.L.; Hermanns, R.C.; Meerman, J.H.; Commandeur, J.N.; Vermeulen, N.P. Disposition in rat of [2-3H]-*trans*-4-hydroxy-2,3-nonenal a product of lipid peroxidation. *Xenobiotica* 26: 1087-1100; 1996.

[60] Stevens, J.F.; Maier, C.S. Acrolein: sources, metabolism, and biomolecular interactions relevant to human health and disease. *Mol. Nutr. Food Res.* 52: 7-25; 2008.

[61] Esterbauer, H.; Weger, W. Über die wirkungen yon aldehyden auf gesunde und maligne zellen. 3. Mitt. *Monatshefte für Chemie* 98: 1995-2000; 1967.

[62] Čorić, I.; Müller, S.; List, B. Kinetic resolution of homoaldols via catalytic asymmetric transacetalization. *J. Am. Chem. Soc.* 132: 17370-17373; 2010.

[63] Ellman, G.L. Tissue sulfhydryl groups. *Arch. Biochem. Biophys.* 82: 70-77; 1959.

[64] Talamo, F.; D'Ambrosio, C.; Arena, S.; Del Vecchio, P.; Ledda, L.; Zehender, G.; Ferrara, L.; Scaloni, A. Proteins from bovine tissues and biological fluids: defining a reference electrophoresis map for liver, kidney, muscle, plasma and red blood cells. *Proteomics* 3: 440-460; 2003.

[65] Salzano, A.M.; Novi, G.; Arioli, S.; Corona, S.; Mora, D.;Scaloni, A. Mono-dimensional blue native-PAGE and bi-dimensional blue native/urea-PAGE or/SDS-PAGE combined with nLC-ESI-LIT-MS/MS unveil membrane protein heteromeric and homomeric complexes in Streptococcus thermophilus. *J. Proteomics* 94:240-261; 2013.

[66] Salzano, A.M. ; Renzone, G.; Scaloni, A.; Torreggiani, A.; Ferreri, C.; Chatgilialoglu, C.Human serum albumin modifications associated with reductive radical stress. *Mol. Biosyst.* 7: 889-898; 2011.

[67] Lirussi,L.; Antoniali, G.; Vascotto, C.; D'Ambrosio, C.; Poletto, M.; Romanello, M.; Marasco, D.; Leone, M.; Quadrifoglio, F.; Bhakat, K.K.; Scaloni, A.; Tell, G. Nucleolar accumulation of APE1 depends on charged lysine residues that undergo acetylation upon genotoxic stress and modulate its BER activity in cells.*Mol Biol Cell*. 23:4079-4096; 2012.

[68] Hwang, T.L.; Shaka, A.J. Water suppression that works: excitation sculpting using arbitrary waveforms and pulse field gradients. *J. Magn. Reson.* 112: 275-279; 1995.

[69] Griesinger, C.; Otting, G.; Wüthrich, K.; Ernst, R.R. Clean TOCSY for proton spin system identification in macromolecules. *J. Am. Chem. Soc.* 110: 7870-7872; 1988.

[70] Kay, L. E.; Keifer, P.; Saarinen, T. Pure absorption gradient enhanced heteronuclear single quantum correlation spectroscopy with improved sensitivity. *J. Am. Chem. Soc.* 114: 10663-10665; 1992.

[71] Bradford, M.M. A rapid and sensitive method for the quantitation of microgram quantities of protein utilizing the principle of protein-dye binding. *Anal. Biochem.* 72: 248-254; 1976.

[72] Laemmli, U.K. Cleavage of structural proteins during the assembly of the head of bacteriophage T4. *Nature* 227: 680-685; 1970.

[73] Wray, W.; Boulikas, T.; Wray, V.P.; Hancock, R. Silver staining of proteins in polyacrylamide gels. *Anal. Biochem.* 118: 197-203; 1981.

[74] Del Corso, A.; Barsacchi, D.; Giannessi, M.; Tozzi, M.G.; Camici, M.; Houben, J.L.; Zandomeneghi, M.; Mura, U. *Arch. Biochem. Biophys.* 283: 512-518; 1990.

[75] Noltmann, E.A.; Gubler, C.J.; Kuby, S.A. Glucose 6-phosphate dehydrogenase (Zwischenferment). I. Isolation of the crystalline enzyme from yeast. *J. Biol. Chem.* 236: 1225-1230; 1961.

[76] Kim, T.K.; Lee, P.; Colman, R.F. Critical role of Lys212 and Tyr140 in porcine NADP-dependent isocitrate dehydrogenase. *J. Biol. Chem.* 278: 49323-49331; 2003.

[77] Betts, S.A.; Mayer, R.J. Purification and properties of 6-phosphogluconate dehydrogenase from rabbit mammary gland. *Biochem. J.* 151: 263-270; 1975.

[78] Schieber, A.; Rainer, W.F.; Ghisla, S. Purification and properties of prostaglandin 9-ketoreductase from pig and human kidney. *Eur. J. Biochem.* 206: 491-502; 1992.

[79] Jarabak, J. Early steps in prostaglandin metabolism in the human placenta. *Am. J. Obstet. Gynecol.* 138: 534-540; 1980.

[80] Ji, B.; Ito, K.; Suzuki, H.; Sugiyama, Y.; Horie, T. Multidrug resistance-associated protein2 (MRP2) plays an important role in the biliary excretion of glutathione conjugates of 4-hydroxynonenal. *Free Radic Biol Med.* 33: 370-378; 2002.

[81] Balogh, L.M.; Roberts, A. G.; Shireman, L. M.; Greene, R.J.; Atkins, W.M. The stereochemical course of 4-hydroxy-2-nonenal metabolism by glutathione S-transferase. *J. Biol. Chem.* 283: 16702-16710; 2008.

[82] Aldini, G.; Carini, M.;Beretta, G.; Bradamante, S.; Facino, R. M. Carnosine is a quencher of 4-hydroxy-nonenal: through what mechanism of reaction?*Biochem. Biophys. Res. Commun*. 298: 699-706; 2002.

[83] Beretta, G.; Artali, R.; Regazzoni, L.; Panigati, M.;Facino, R.M. Glycyl-histidyl-lysine (GHK) is a quencher of alpha,beta-4-hydroxy-trans-2-nonenal: a comparison with carnosine. Insights into the mechanism of reaction by electrospray ionization mass spectrometry, 1H NMR, and computational techniques. *Chem. Res. Toxicol*. 20:1309-1314; 2007.

[84] Xie, C.; Zhong, D.; Chen, X. A fragmentation-based method for the differentiation of glutathione conjugates by high-resolution mass spectrometry with electrospray ionization. *Anal. Chim. Acta* 788: 89-98; 2013.

[85] Wermuth, B. Purification and properties of an NADPH-dependent carbonyl reductase from human brain. Relationship to prostaglandin 9-ketoreductase and xenobiotic ketone reductase. *J. Biol. Chem.* 256: 1206-1213; 1981.

[86] Hoffmann, F.; Maser, E. Carbonyl reductases and pluripotent hydroxysteroid dehydrogenases of the short-chai dehydrogenase/reductase superfamily. *Drug Metab. Rev*. 39: 87-144; 2007.

[87] Doorn, J.A.; Maser, E.; Blum, A.; Claffey, D.J.; Petersen, D.R. Human carbonyl reductase catalyzes reduction of 4-oxonon-2-enal. *Biochemistry* 43: 13106-13114; 2004.

[88] Forrest, G.L.; Gonzalez, B. Carbonyl reductase. *Chem. Biol. Interact.* 129: 21-40; 2000.

[89] Kelner, M.J.; Estes, L.; Rutherford, M.; Uglik, S.F.; Peitzke, J.A. Heterologous expression of carbonyl reductase: demonstration of prostaglandin 9-ketoreductase activity and paraquat resistence. *Life Sci.* 61: 2317-2322; 1997.

[90] Maser, E. Neuroprotective role for carbonyl reductase? *Biochem. Biophys. Res. Commun.* 340: 1019-1022; 2006.

[91] Kim, Y.N.; Jung, H.Y.; Eum, W.S.; Kim, D.W.; Shin, M.J.; Ahn, E.H.; Kim, S.J.; Lee, C.H.; Yong, J.I.; Ryu, E.J.; Park, J.; Choi, J.H.; Hwang, I.K.; Choi, S.Y. Neuroprotective effects of PEP-1-carbonyl reductase 1 against oxidative-stress-induced ischemic neuronal cell damage. *Free Rad. Biol. Med.* 69: 181-196; 2014.

[92] Rashid, M.A.; Lee, S.; Tak, E.; Lee, J., Choi, T.G.; Lee, J.W.; Kim, J.B.; Youn, J.H.; Kang, I.; Ha, J.; Kim, S.S. Carbonyl reductase 1 protects pancreatic β-cells against oxidative stress-induced apoptosis in glucotoxicity and glucolipotoxicity. *Free Rad. Biol. Med.* 49: 1522-1533; 2010.

[93] Bateman, R.L.; Rauh, D.; Tavshanjian, B.; Shokat, K.M. Human carbonyl reductase 1 is an S-nitrosoglutathione reductase. *J. Biol. Chem.* 283: 35756-35762; 2008.

[94] Krook, M.; Ghosh, D.; Strömberg, R.; Carlquist, M.; Jörnvall, H.; Carboxyethyllysine in a protein: native carbonyl reductase/NADP($^{+}$)-dependent prostaglandin dehydrogenase. *Proc. Natl. Acad. Sci.* 90: 502-506; 1993.

[95] Sciotti, M.A.; Nakajin, S.; Wermuth, B.; Baker, M.E. Mutation of threonine-241 to proline eliminates autocatalytic modification of human carbonyl reductase. *Biochem. J.* 350: 89-92; 2000.

[96] Iwata, N.; Inazu, N.; Satoh, T. The purification and properties of NADPH-dependent carbonyl reductases from rat ovary. *J. Biochem.* 105: 556-564; 1989.

[97] Ahmad, I.M.; Aykin-Burns, N.; Sim, J.E.; Walsh, S.A.; Higashikubo, R.; Buettner, G.R.; Venkataraman, S.; Mackey, M.A.; Flanagan, S.W.; Oberley, L.W.; Spitz, D.R. Mitochondrial O_2- and H_2O_2 mediate glucose deprivation-induced stress in human cancer cells. *J. Biol. Chem.* 280: 4254-4263; 2005.

[98] Aykin-Burns, N.; Ahmad, I.M.; Zhu, Y.; Oberley, L.W.; Spitz, D.R. Increased levels of superoxide and H_2O_2 mediate the differential susceptibility of cancer cells versus normal cells to glucose deprivation. *Biochem. J.* 418: 29-37; 2009.

[99] Cairns, R.A.; Harris, I.S.; Mak, T.W. Regulation of cancer cell metabolism. *Nat. Rev. Cancer* 11: 85-95; 2011.

Figure captions

Figure 1. Double reciprocal plot for the reduction of 9,10-PQ by CBR1.

The initial rate measurements of the NADPH-dependent reduction of 9,10-PQ are reported as double reciprocal plot. The assays were performed in standard conditions using 1.2 mU/mL of purified CBR1. Error bars represent the standard deviations of the mean from at least three independent measurements.

Figure 2.Kinetic analysis of the $NADP^+$ dependent dehydrogenase activity of CBR1.

The initial rate measurements of the $NADP^+$-dependent oxidation of GSHNE (panel A) and PGB_1 (panel B) are reported as double reciprocal plot. The assays were performed in standard conditions using 2.3 mU/mL and 4.6 mU/mL of purified CBR1, respectively. Error bars represent the standard deviations of the mean from at least three independent measurements.

Figure 3. Cofactor specificity of CBR1.

The initial rate of GSHNE oxidation measured at the indicated concentrations of $NADP^+$ alone (closed circles), or in the presence of either 10 μM NADPH (squares) or10 μM of NAD^+(triangles) are reported as double reciprocal plot. The assays were performed in standard conditions using2.3 mU/mL of purified CBR1. Error bars represent the standard deviations of the mean from at least three independent measurements.

Figure 4. Fragmentation spectra of the GSH derivatives observed in this study after their collision induced dissociation in positive polarity.

The fragment nomenclature is identical to that described in Xie et *al*. [84]. In particular, a=P-75.032, b=145.061, c=P-146.069, d=P-273.096 or 275.112, e=P-129.043, f=130.050, g=P-232.070, h= P-249.095, I =308.091, j=P-307.084 or 305.068, k=274.103, where P represents the $[M+H]^+$ ion of the specific GSH conjugate. Panels A, B, C and D show the fragmentation spectrum of the species showing a $[M+H]^+$ ion at the experimental *m/z* value 464.18, 462.23, 480.25 and 478.19, respectively. R_1, R_2, R_3 and R_4 represent the corresponding neutral losses of $C_9H_{16}O_2$ (156.12 Da), $C_9H_{14}O_2$ (154.10 Da), $C_9H_{16}O_3$ (172.11 Da) and $C_9H_{14}O_3$ (170.09 Da), respectively. Apart from the most intense peak in each presented spectrum, the other regions in the spectra were magnified by a factor of 10. To obtain a more certain assignation of the MS^2 spectra, several experiments of MS^3 fragmentation were also performed. As an example, Supplementary Fig. 7S shows the MS^3 experiment of the peak at *m/z* 446.07 in the MS^2 spectrum of the original species at *m/z* 464.18, which was assigned to the neutral loss of a single water molecule from the parent ion.

Figure 5. Time course of GSHNE oxidation catalyzed by CBR1.

Plots of peak areas of the species detected at *m/z* values 464.18, 462.23, 480.25 and 478.19 at different times of incubation with CBR1 (panels A to D, respectively), as obtained by the integration of the corresponding extracted ion currents in LC-MS runs.

Figure 6. Proposed reaction pathway catalyzed by CBR1.

The scheme reports possible reaction pathways as deriving from the nature of the products observed during time-course nLC-ESI-LIT-MS/MS and NMR analyses of the incubation mixtures.

Figure 7. NMR spectra of single products and their mixtures in phosphate buffer.

In the GSHNE-GSH-HNE and GSHNE-GSH-HNE-$NADP^+$ spectra (upper and middle), the envelope centered at 5.57 ppm was assigned to proton 1 of GSHNE. Four peaks (I at 5.59 ppm, II at 5.53 ppm, III at 5.50 ppm, and IV at 5.47 ppm) were identified. The remaining proton signals of GSHNE were also identified and labeled.

Figure 8. NMR spectra of time course reaction with CBR1 in phosphate buffer. The low field region indicates that, in the presence of CBR1, peaks I-IV originating from proton 1 of GSHNE start to be modified after 10 min, with all NADPH peaks appearing and the corresponding reduction of NAD^+. After 80 min peaks II, III and IV almost disappeared, while peak I was still partially present, with the doublet at 5.50 ppm originating from NADPH. After 155 min (top spectrum) peak I was barely visible.

Figure 9. Lactone identification during the time course reaction with CBR1 in phosphate buffer.

The region between 2.5 and 2.3 ppm comprises the signal of proton 2 of GSHNE. The ongoing reaction from 10 min to 155 min indicates that the multiplicity of proton 2 changes from a multiplet (at 10 min) to become a double doublet (at 80 min). This multiplicity originates from the coupling with proton 3, while coupling with proton 1 is removed by lactone formation.

Highlights

1) Glutathionyl-hydroxynonanal is susceptible to $NADP^+$-dependent oxidation catalyzed by carbonyl reductase.

2) The glutathionyl-4-hydroxynonanoic acid δ-lactone is the main product of the reaction.

3) The reaction may lead to hydroxynonenal detoxification while recovering cell reducing power.

Table 1 Substrate specificity of the NADPH-dependent reductase activity of carbonyl reductase.[a]

Substrate	Concentration (μM)	Relative activity (%)[b]
9,10-phenanthrenquinone	40	100
Menadione	250	48
4-oxo-nonenal	1000	9
HNE, GSHNE, glutathione-nonanal, *trans*-2-nonenal[c].	100	n.d.[d]

[a]Enzyme activity was measured as described under Materials and Methods section at the indicated substrate concentrations.

[b]Hundred % of enzyme activity refers to 1.2 mU/mL.

[c]Each compound was individually tested.

[d]n.d. stands for not detectable.

Table 2. Substrate specificity for the $NADP^+$-dependent dehydrogenase activity of CBR1.[a]

Substrate	Relative rate (%)[b]
GSHNE	100
PGB_1	18
HNE, 4-hydroxynonanal, 4-oxo-nonenal, *trans*-2-nonenal, CysHNE, CysGlyHNE, γ-GutCysHNE , mercapturic acid-HNE, GS-nonanal[c].	n.d.[d]

[a]Substrate concentration in the assay mixture was 100 μM, with the only exception for PGB_1 present at 450 μM.

[b]Hundred % activity refers to 2.3 mU/mL.

[c]Each compound was individually tested.

[d]n.d. stands for not detectable.

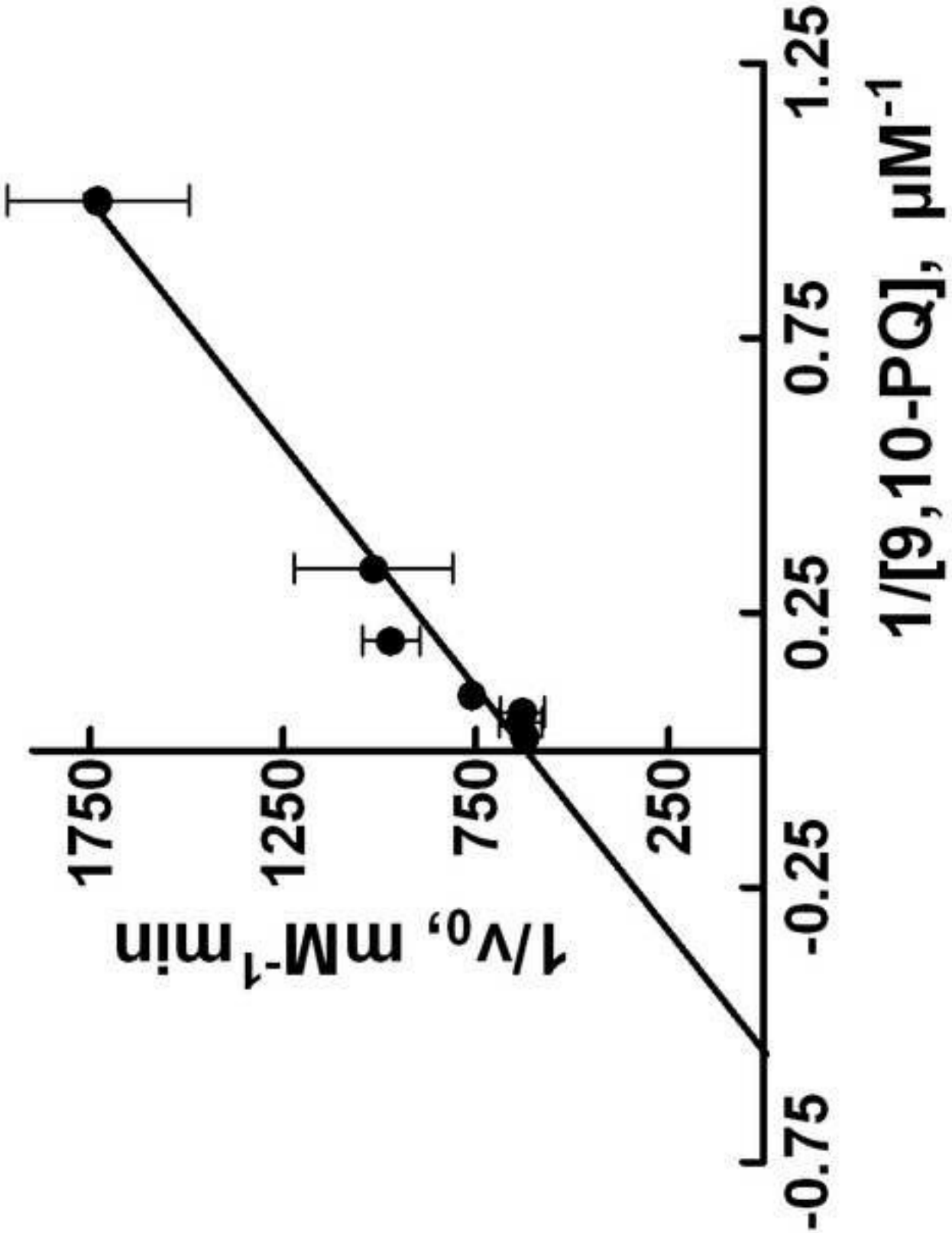

Figure 1

Figure 2

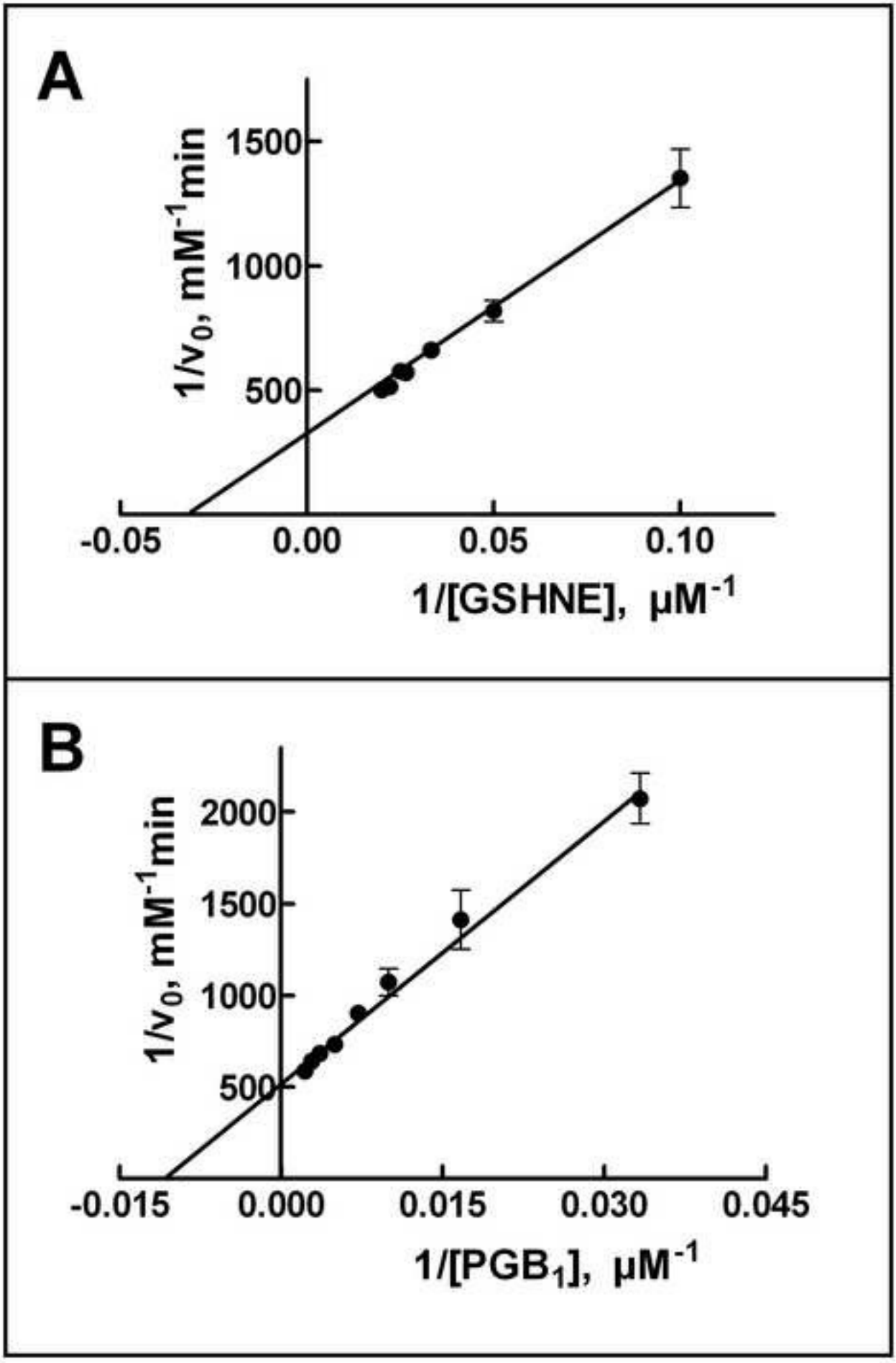

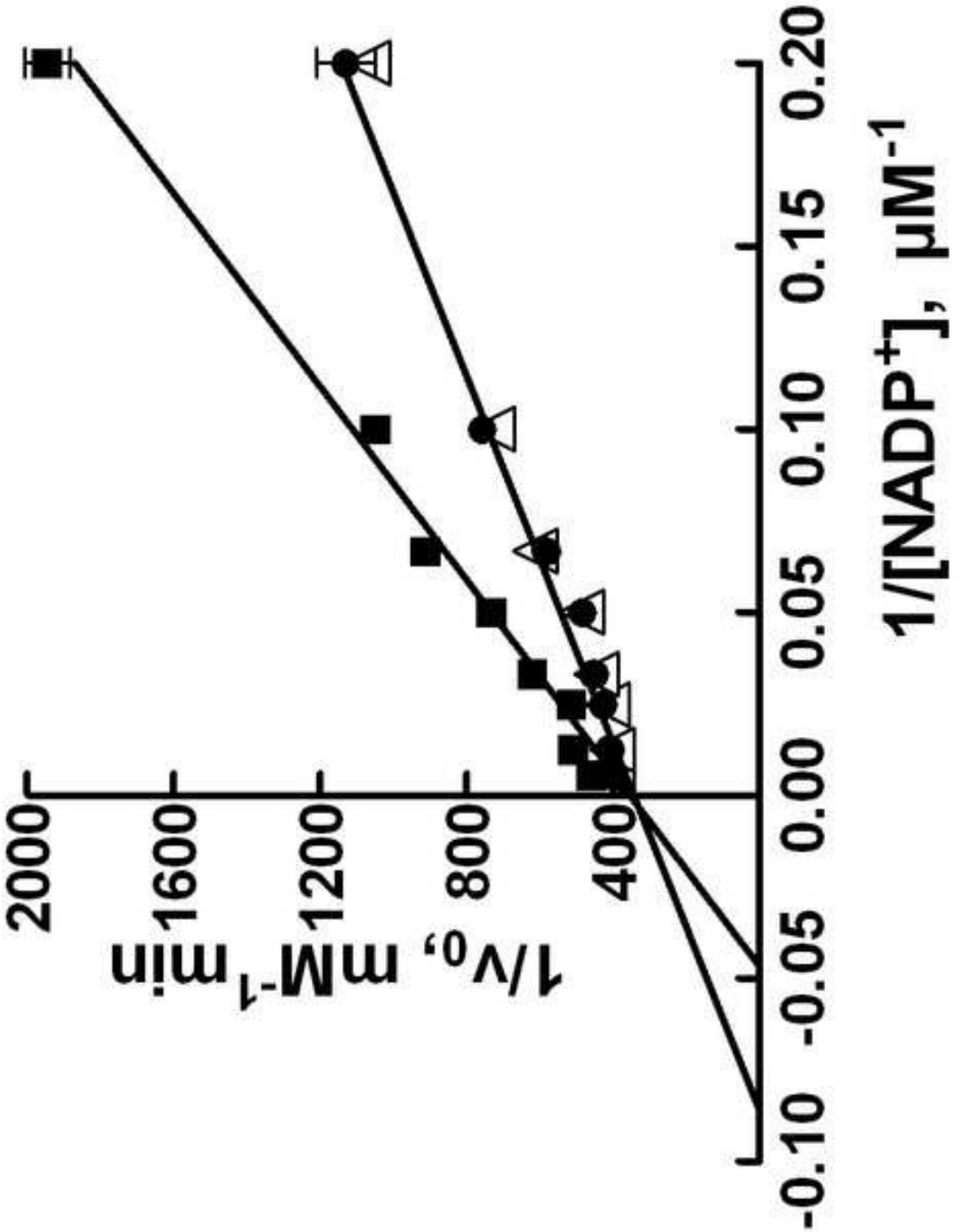

Figure 3

Figure 4

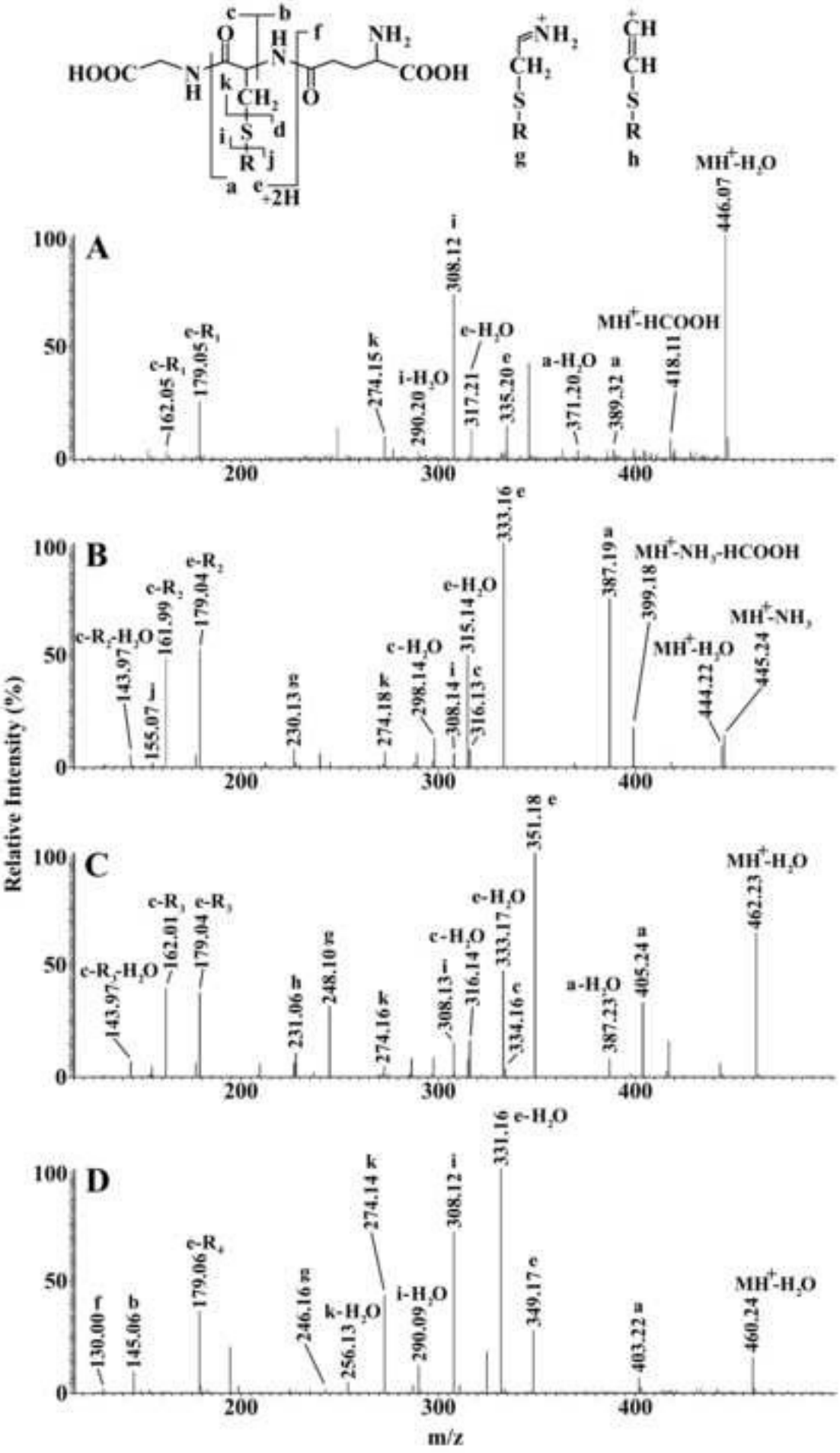

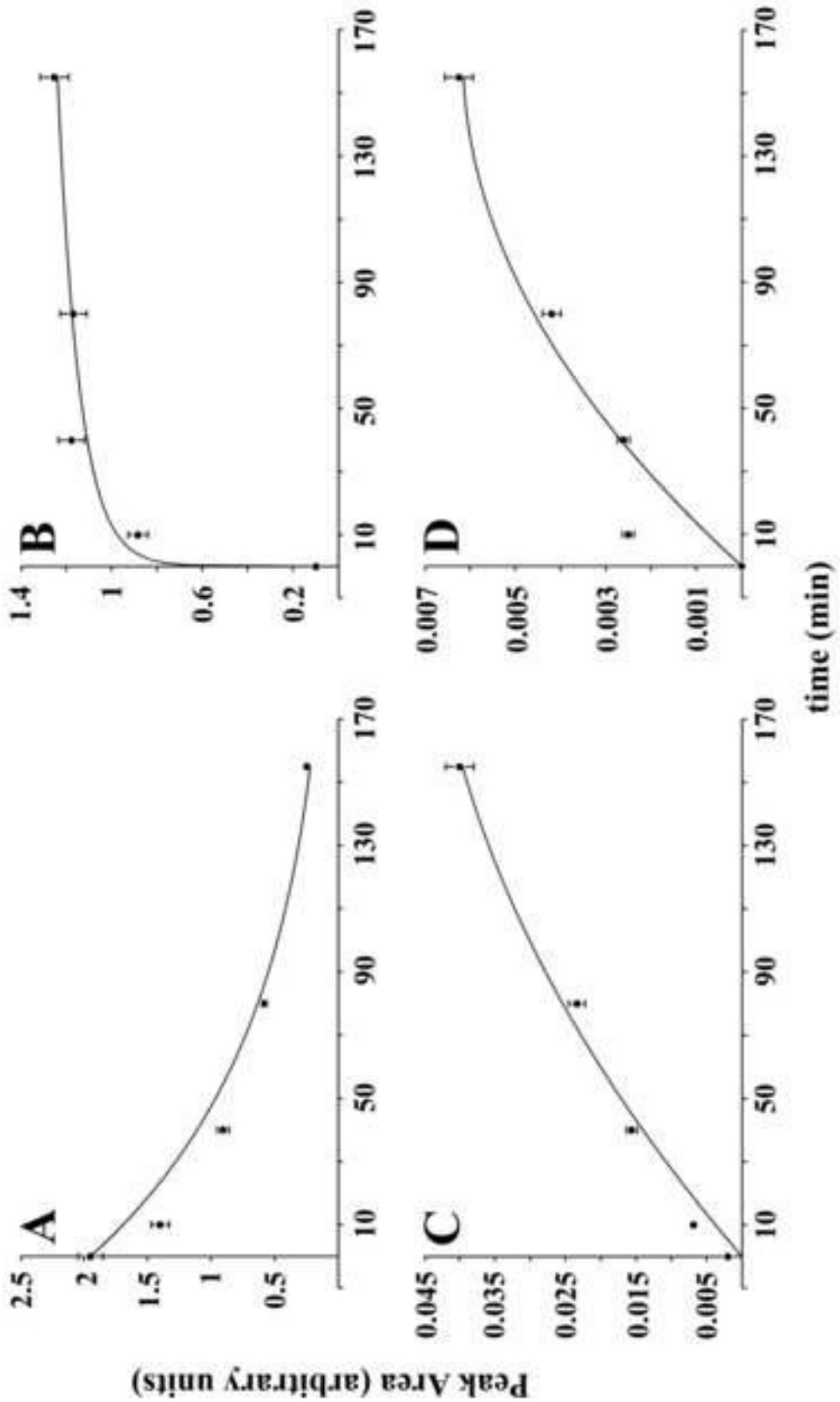

Figure 5

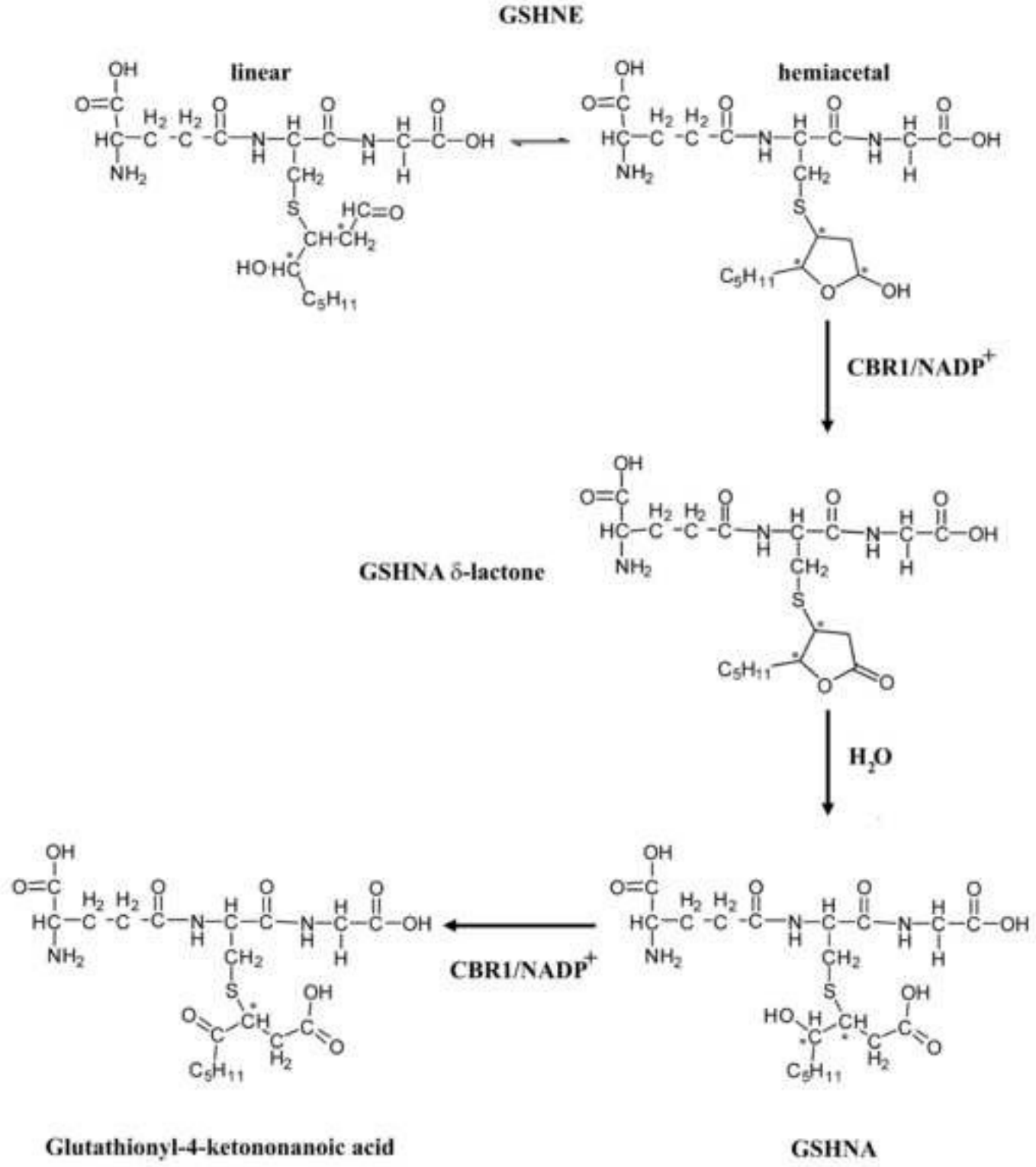

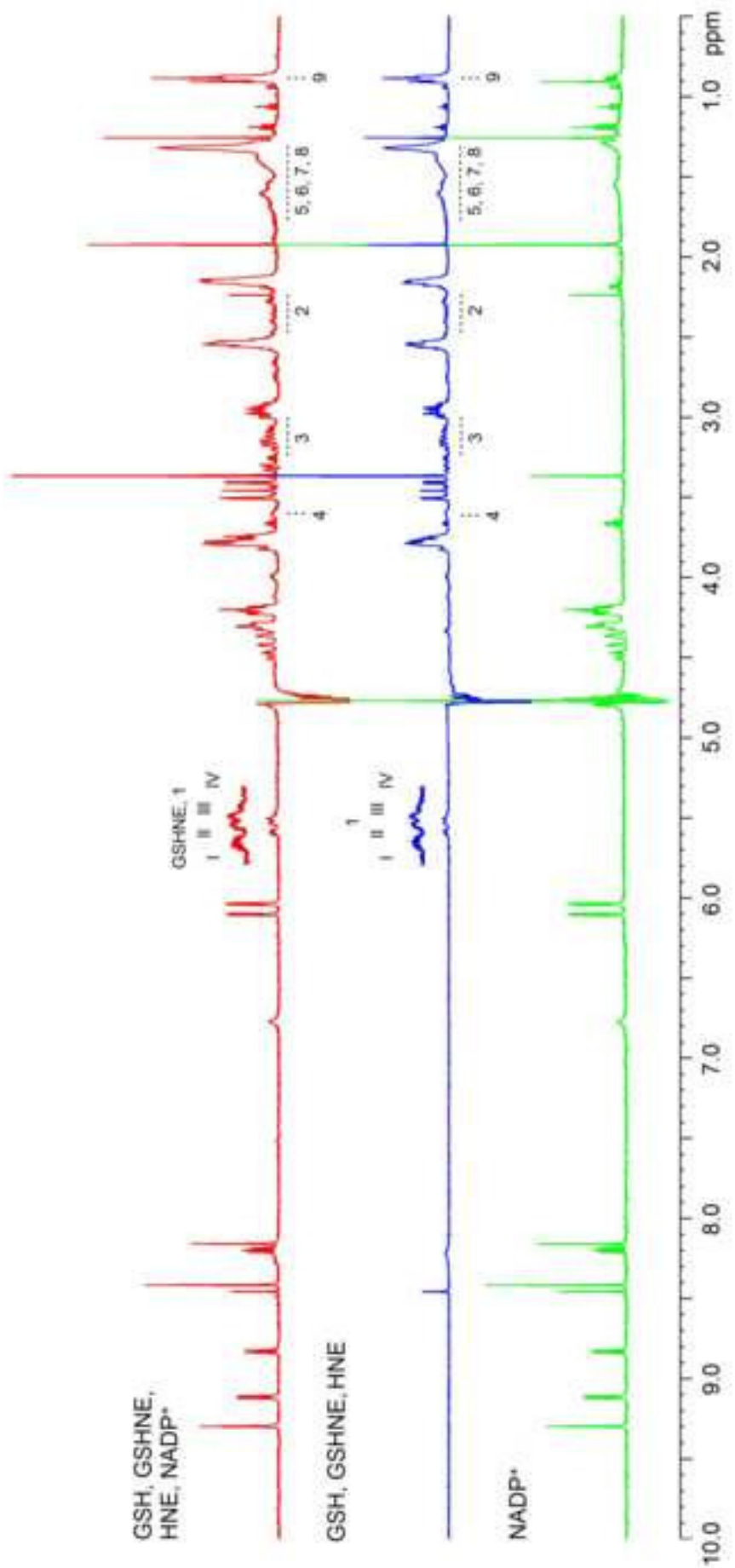
GSH, GSHNE, HNE, NADP+
GSH, GSHNE, HNE
NADP+
GSHNE, 1
I II III IV
1
I II III IV
4
3
2
5, 6, 7, 8
9
10.0
9.0
8.0
7.0
6.0
5.0
4.0
3.0
2.0
1.0 ppm

Figure 7

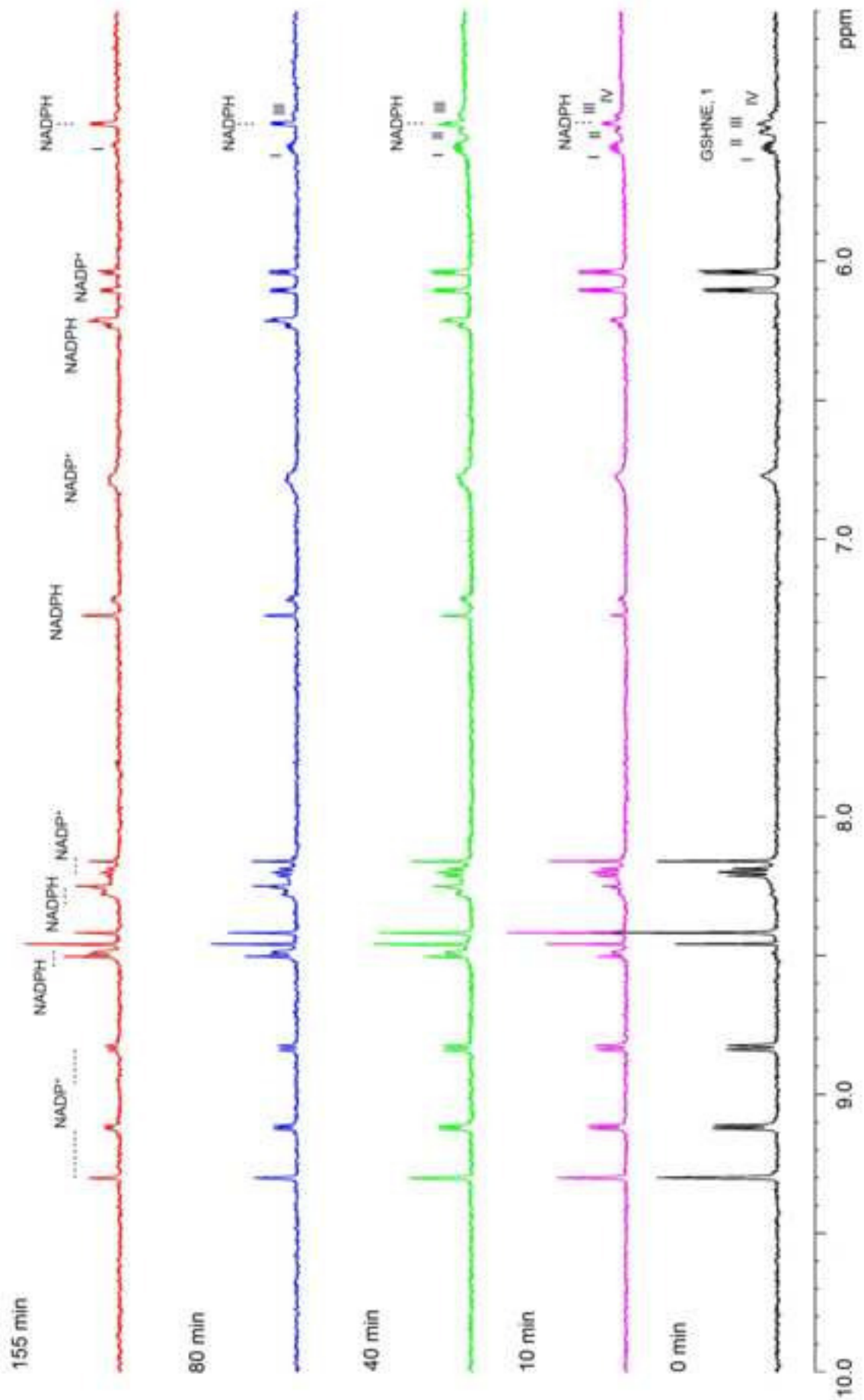
155 min
80 min
40 min
10 min
0 min
NADP+
NADPH
NADPH
NADP+
NADPH
NADP+
NADPH
NADP+
NADPH
I
I III
I II III
I II III IV
GSHNE, 1
I II III IV
10.0
9.0
8.0
7.0
6.0
ppm

Figure 8

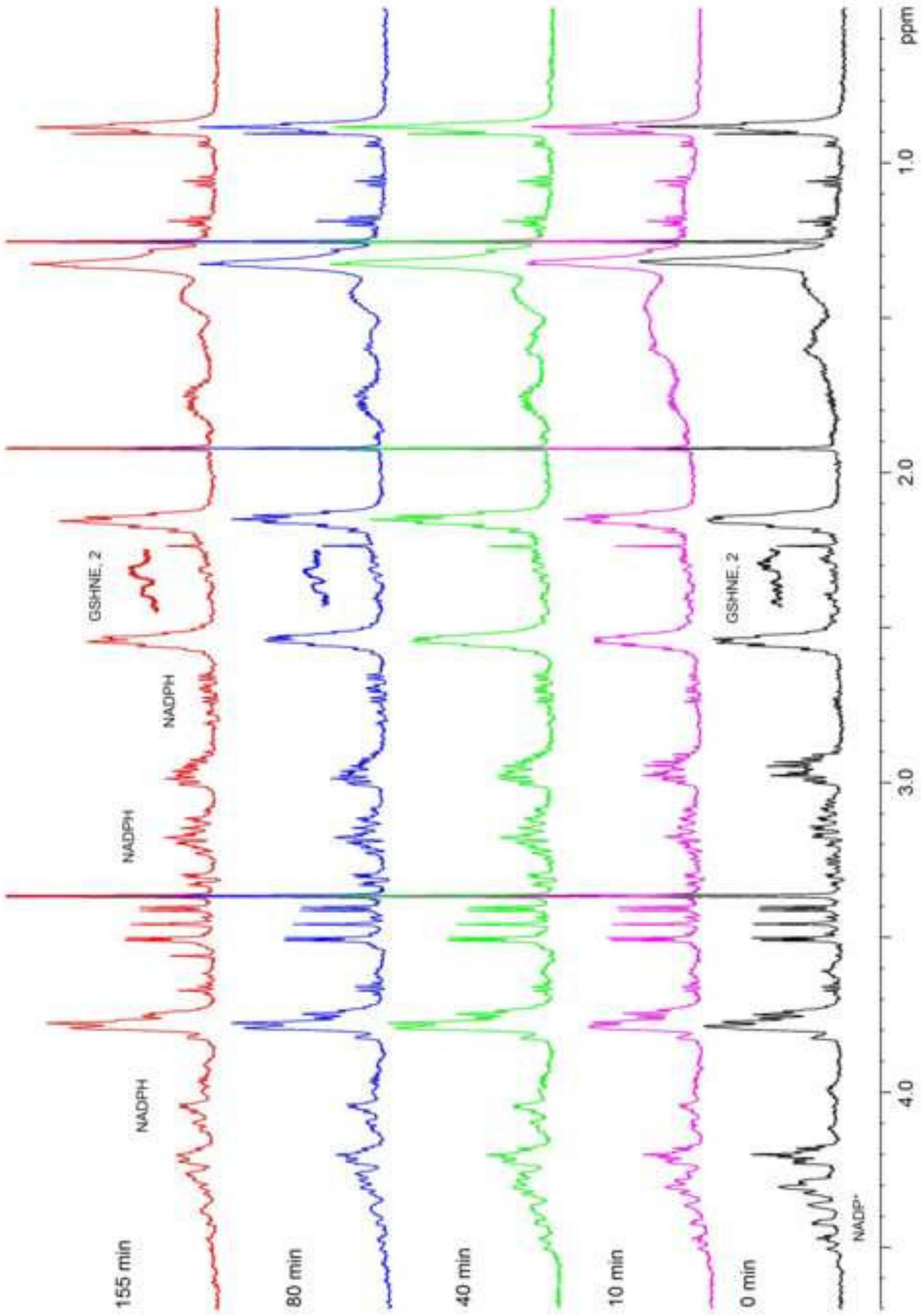

Figure 9

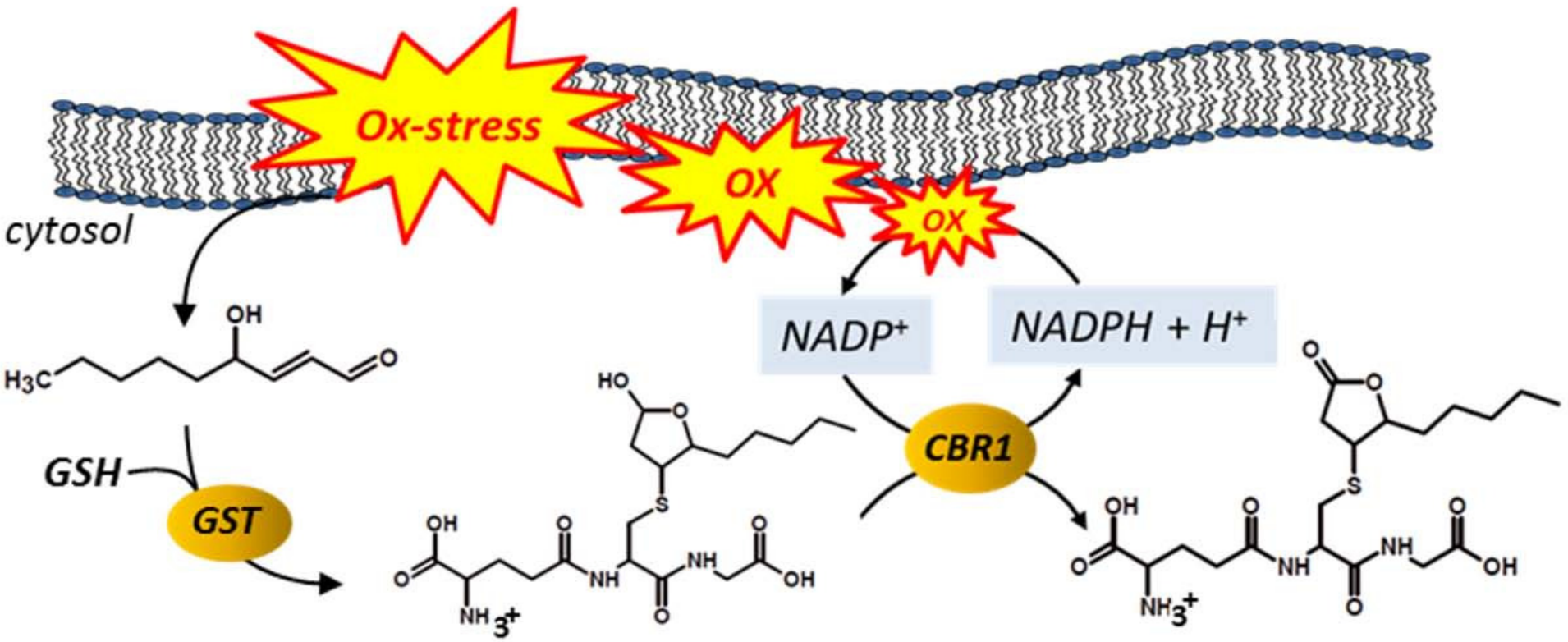
Ox-stress
OX
OX
cytosol
OH
H3C
O
GSH
GST
NADP+
NADPH + H+
CBR1
HO
O
S
OH
O
NH
NH
OH
NH3+
O
OH
O
NH
NH
OH
NH3+